

Symmetry energy, unstable nuclei, and nuclear pasta

Kei Iida (Kochi Univ.)

Kazuhiro Oyamatsu (Aichi Shukutoku Univ.)

Contents

Introduction

Nuclear radii and the EOS of nuclear matter

Nuclear masses and the EOS of nuclear matter

Neutron star crusts and the EOS of nuclear matter

Conclusion

Introduction

Contents

Systems composed of nuclear matter

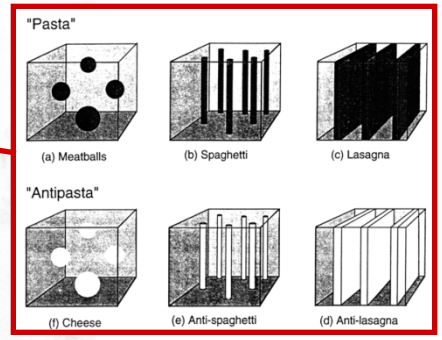
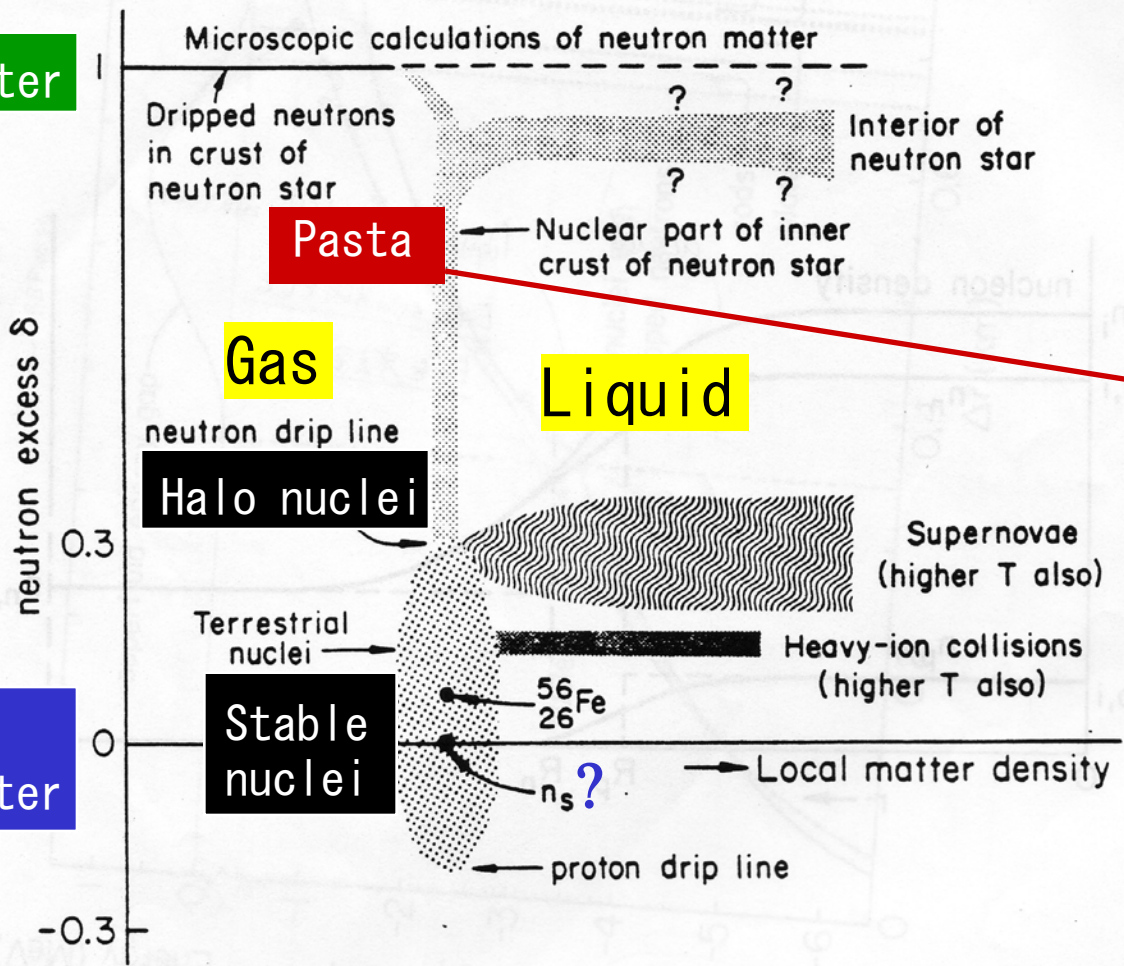
Phenomenological EOS parameters

Microscopic EOS calculations

Systems composed of nuclear matter

Neutron matter

Symmetric nuclear matter



From Lamb (1991).

Phenomenological EOS parameters

Energy per nucleon of bulk nuclear matter near the saturation point
(nucleon density n , neutron excess α):

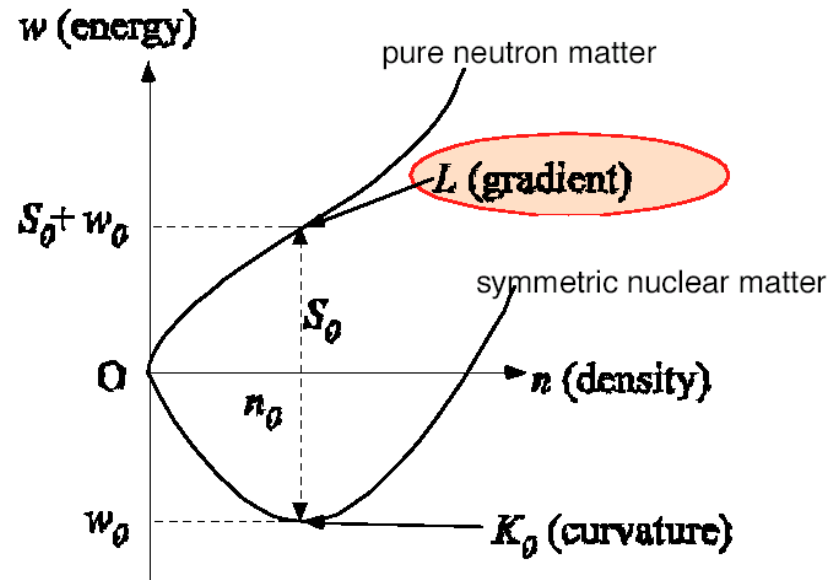
$$w = w_0 + \frac{K_0}{18n_0^2}(n - n_0)^2 + \left[S_0 + \frac{L}{3n_0}(n - n_0) \right] \alpha^2$$

n_0, w_0 saturation density & energy of symmetric nuclear matter

S_0 symmetry energy coefficient

K_0 incompressibility

L density symmetry coefficient

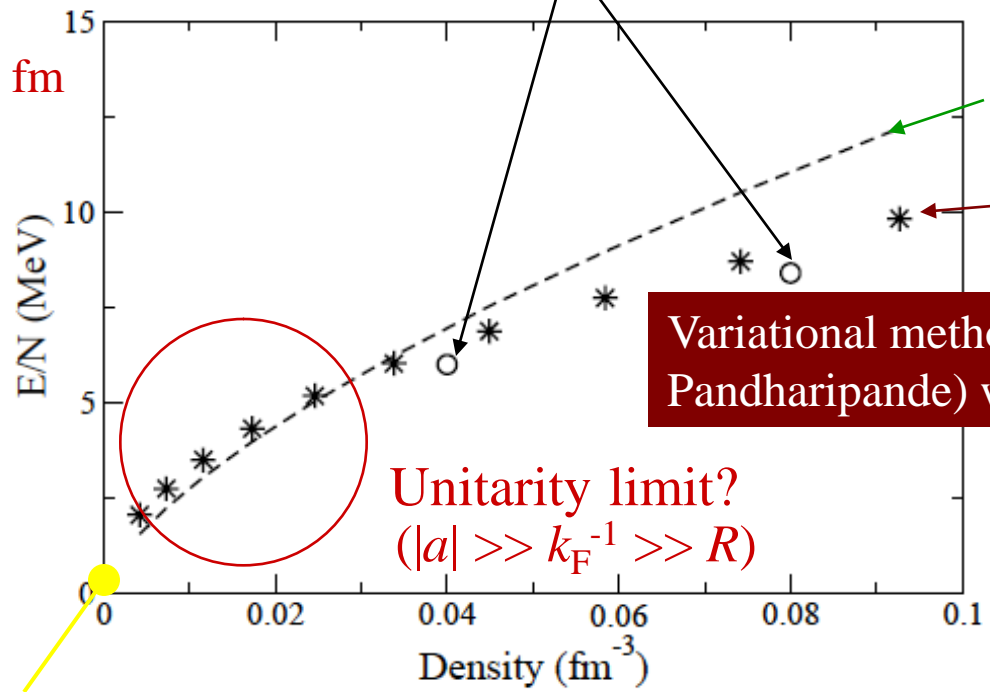


Microscopic EOS calculations

Pure neutron matter

Scattering length $a \approx -18$ fm
 Effective range $R \approx 2$ fm

Green's function Monte-Carlo (GFMC)
 with Argonne v_8'



$0.5 E_{FG}/N$

Variational method (Friedman-Pandharipande) with Urbana v_{14} +TNI

Unitarity limit?
 $(|a| \gg k_F^{-1} \gg R)$

Low - density expansion :

$$E = E_{FG} \left[1 + \frac{10}{9\pi} k_F a + \frac{4}{21\pi^2} (11 - 2\ln 2) (k_F a)^2 + \dots \right]$$

Ref. Carlson et al., PRC **68** (2003) 025802.

Symmetric nuclear matter

Variational method: Overbinding without **phenomenological three-nucleon forces**

Nuclear radii and the equation of state of nuclear matter

Question

Can we extract the saturation properties of asymmetric nuclear matter from the size of unstable nuclei?

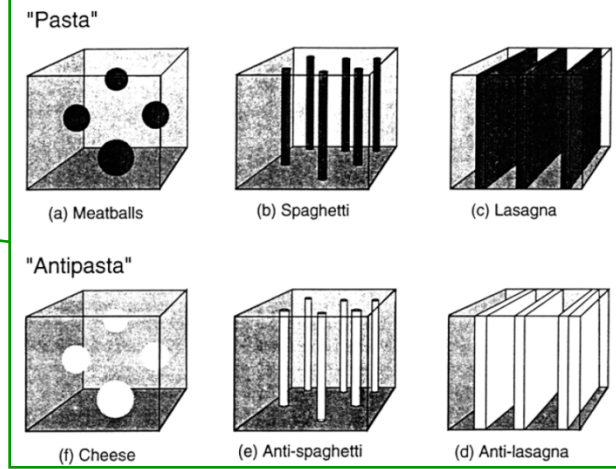
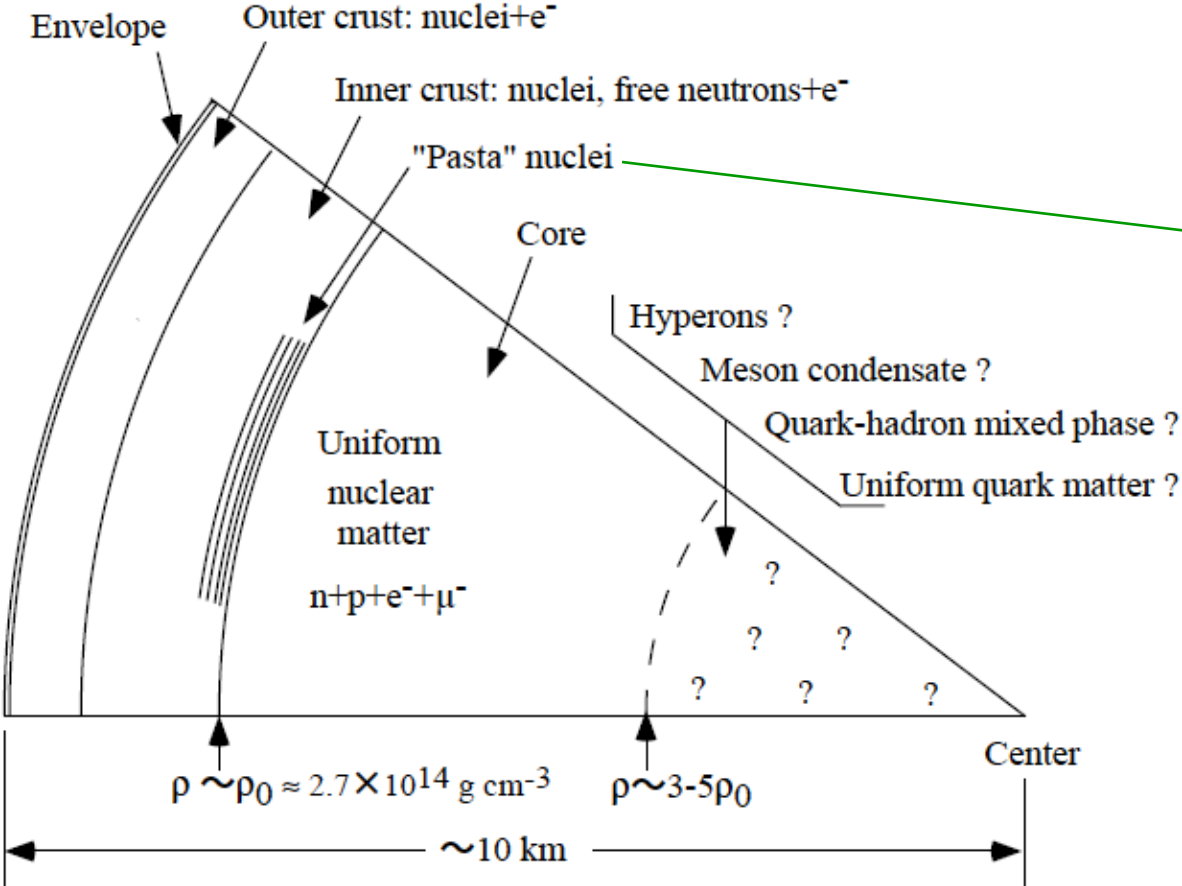
Contents

Motivation

Phenomenological EOS model

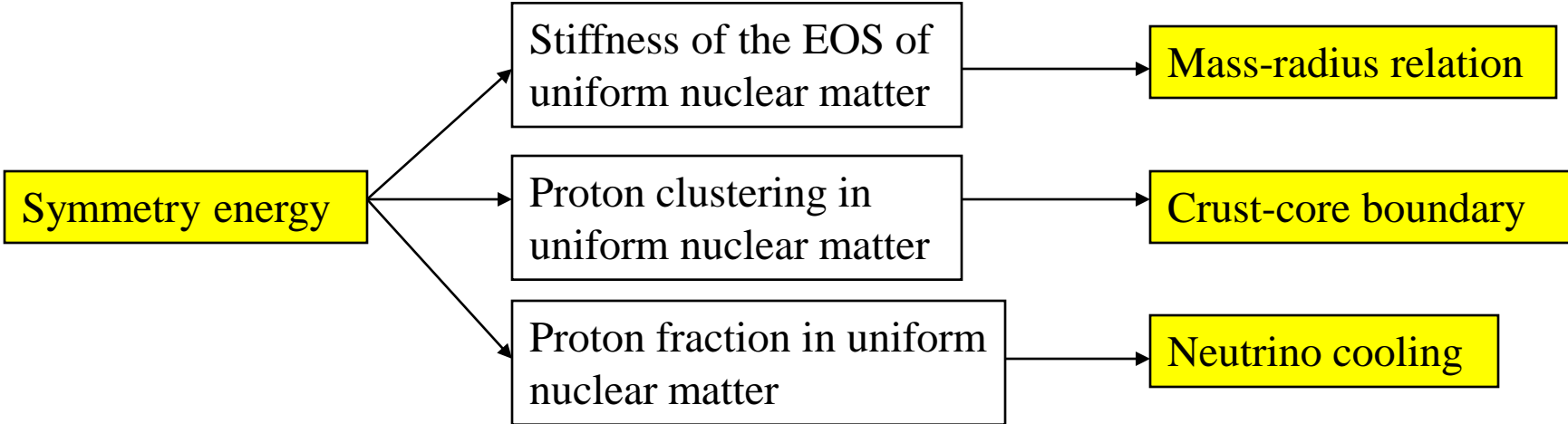
Macroscopic nuclear model

Short summary



From Lamb (1991).

Schematic cross-section of a neutron star.



Motivation

Nuclear matter properties

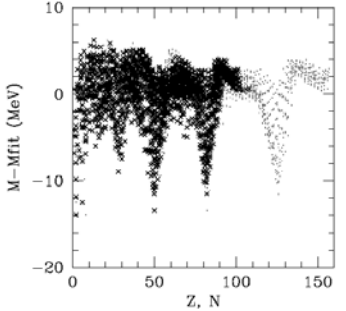
Observables

- Saturation of density and binding energy Masses and radii of stable nuclei

Weizsäcker-Bethe mass formula

$$-E_B = E_{\text{vol}} + E_{\text{sym}} + E_{\text{sur}} + E_{\text{Coul}}$$

E_{vol} : Saturation energy of symmetric nuclear matter
 E_{sym} : Symmetry energy
 E_{sur} : Surface energy



- Incompressibility Giant monopole resonances in stable nuclei

$$K_0 = 9(dP/dn)_{n=n_0}$$

Ref. Blaizot, Phys. Rep. **64** (1980) 171.

Caloric curves in nuclear collisions
 Ref. Natowitz et al., PRL **89** (2002) 212701.

Our focus:

- Density derivative of the symmetry energy Radii of *unstable* nuclei

Ref. Oyamatsu & Iida, PTP **109** (2003) 631.

$$L = 3n_0(dS/dn)_{n=n_0}$$

How can one deduce the radii of unstable nuclei from possible future elastic scattering experiments using a radioactive ion beam incident on a proton target?

Ref. Kohama, Iida, & Oyamatsu, PRC **69** (2004) 064316.

Phenomenological EOS model

• Energy per nucleon of bulk nuclear matter (nucleon density n , proton fraction x)

$$w = \frac{3\hbar^2(3\pi^2)^{2/3}}{10mn} (n_n^{5/3} + n_p^{5/3}) + (1-\alpha^2)v_s(n)/n + \alpha^2 v_n(n)/n$$

$$v_s = a_1 n^2 + \frac{a_2 n^3}{1+a_3 n}, \quad v_n = b_1 n^2 + \frac{b_2 n^3}{1+b_3 n}, \quad \alpha = 1-2x, \quad n_p = nx, \quad n_n = n(1-x)$$

Near the saturation point of symmetric nuclear matter ($n \rightarrow n_0, \alpha \rightarrow 0$)

$$w = w_0 + \frac{K_0}{18n_0^2} (n - n_0)^2 + \left[S_0 + \frac{L}{3n_0} (n - n_0) \right] \alpha^2$$

n_0, w_0	saturation density & energy of symmetric nuclear matter	}
S_0	symmetry energy coefficient	
K_0	incompressibility	
L	density symmetry coefficient	

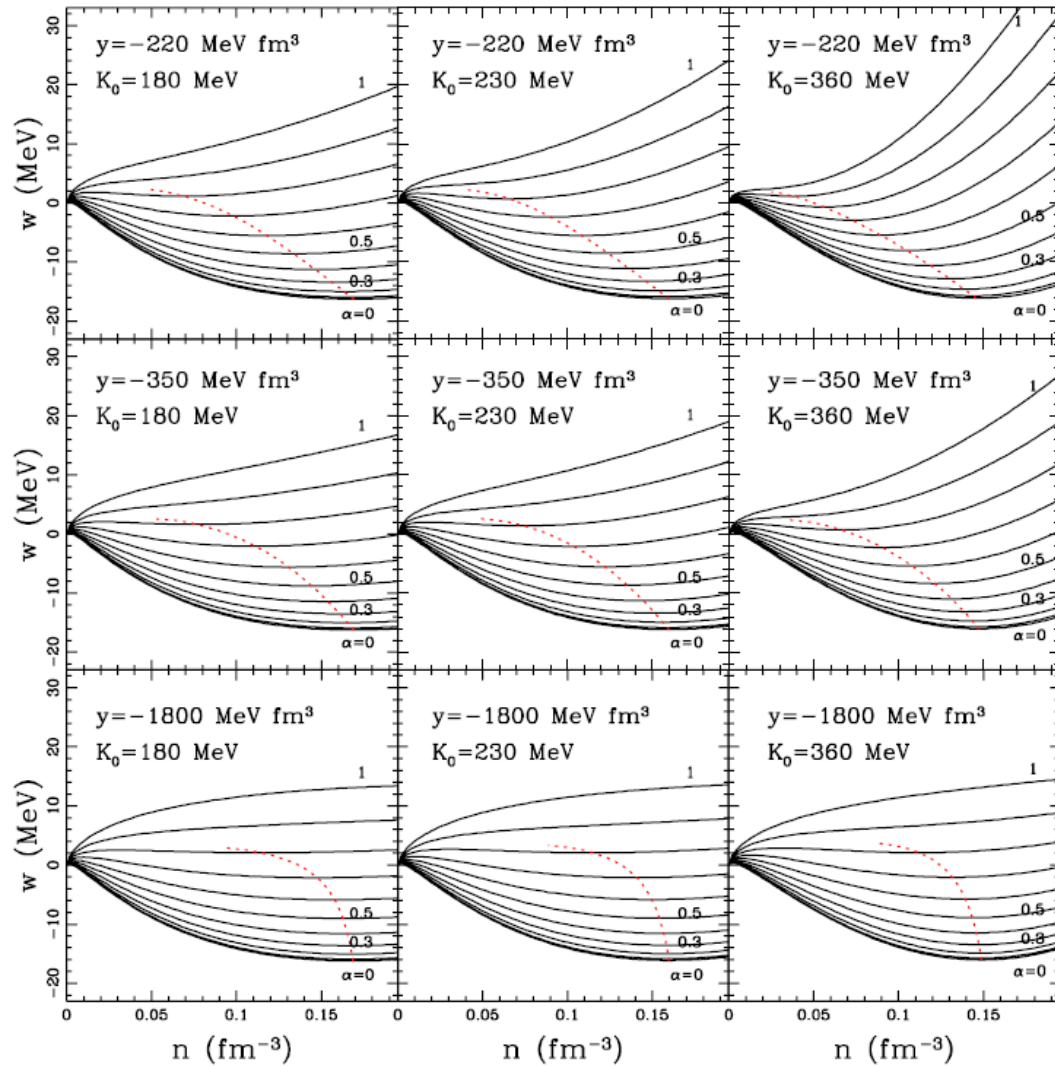
well known from masses and radii of stable nuclei



mainly determine the saturation points at finite neutron excess as

$$n_s = n_0 - \frac{3n_0 L}{K_0} \alpha^2$$

$$w_s = w_0 + S_0 \alpha^2$$

K_0 L 

..... saturation line

$(y = -K_0 S_0 / 3n_0 L : \text{slope at } \alpha = 0)$

Macroscopic nuclear model

- Binding energy of a nucleus

$$-E_B = \int d^3r n(\mathbf{r}) w(n_n(\mathbf{r}), n_p(\mathbf{r})) + F_0 \int d^3r |\nabla n(\mathbf{r})|^2 + \frac{e^2}{2} \int d^3r \int d^3r' \frac{n_p(\mathbf{r}) n_p(\mathbf{r}')}{|\mathbf{r} - \mathbf{r}'|}$$

- Particle distributions ($i=n, p$)

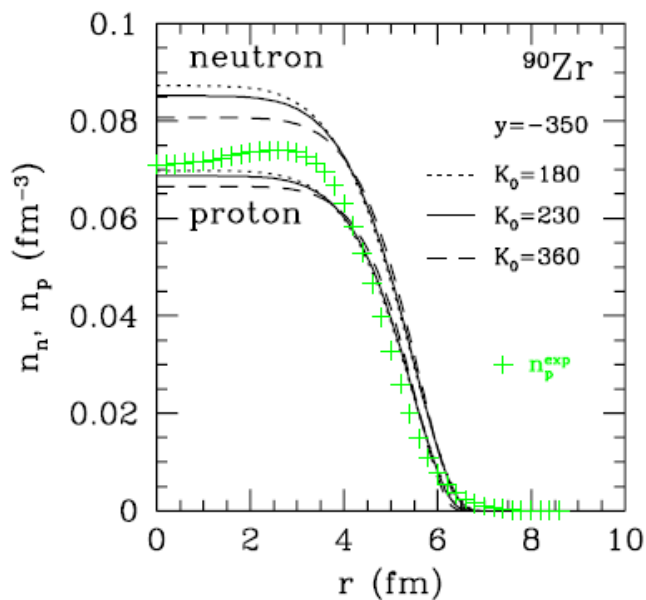
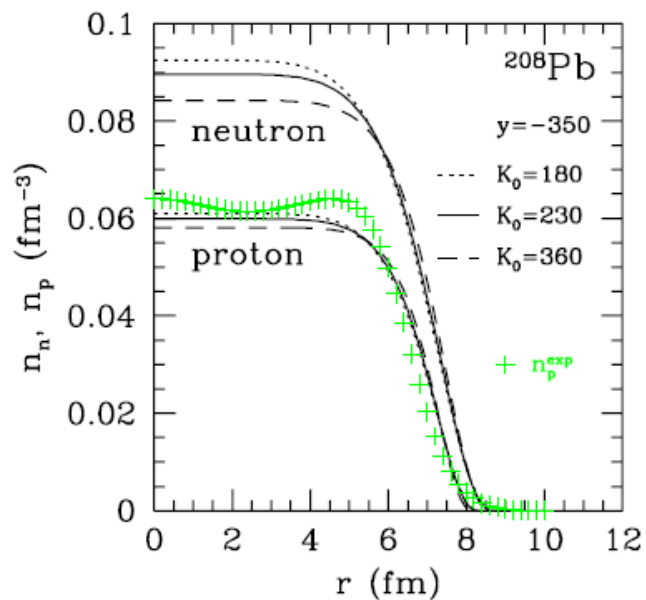
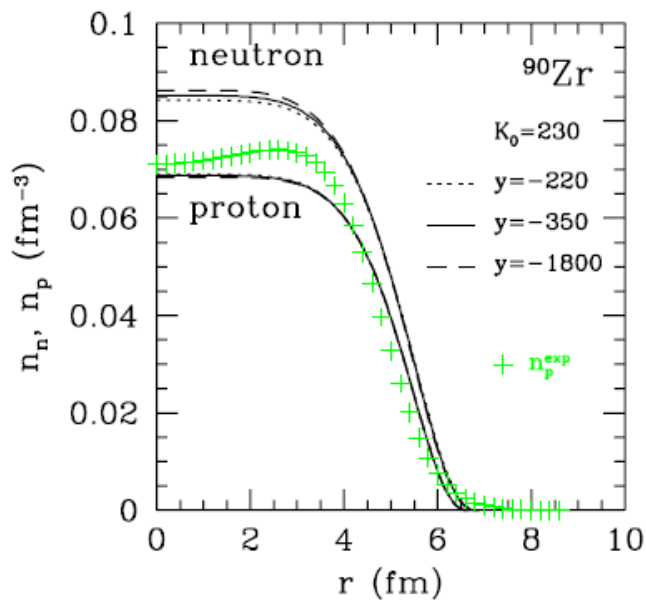
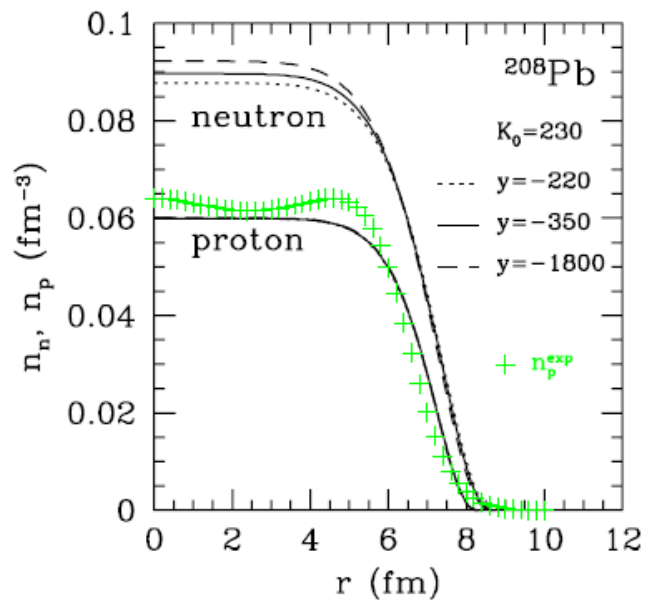
$$n_i(r) = \begin{cases} n_i^{\text{in}} \left[1 - (r/R_i)^{t_i} \right]^3, & r < R_i \\ 0, & r \geq R_i \end{cases}$$

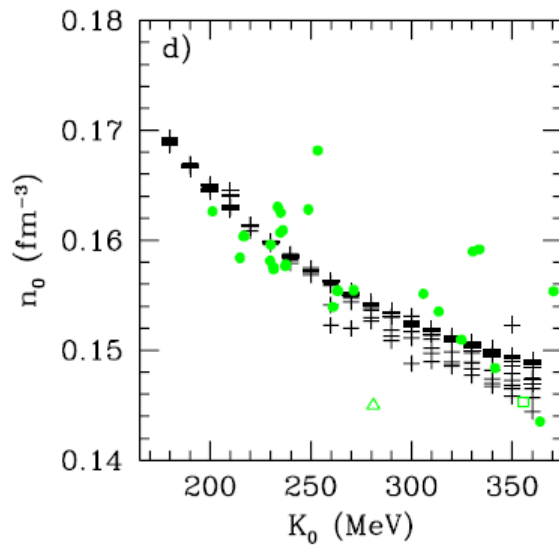
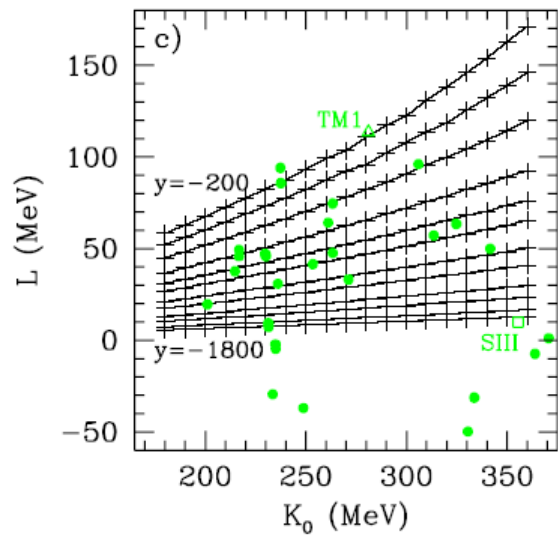
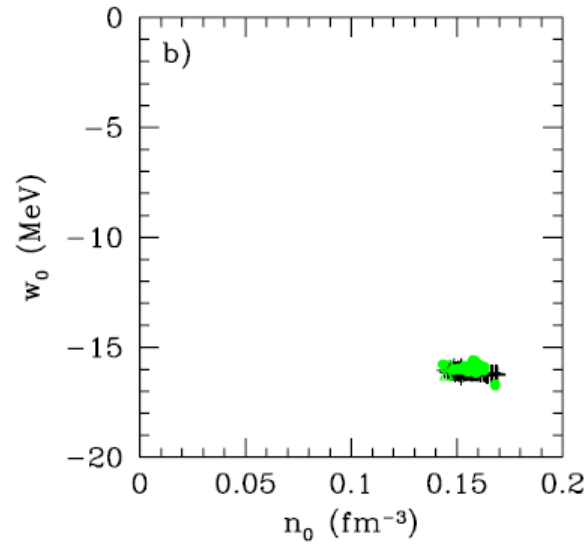
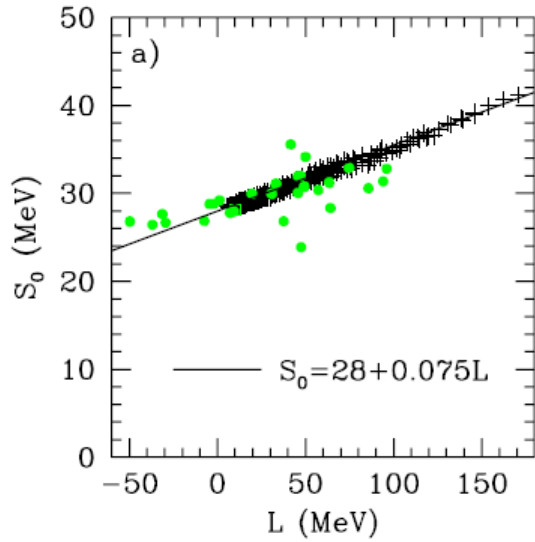
1. Thomas-Fermi approximation Ref. Oyamatsu, NPA **561** (1993) 431.

extremize the binding energy E_B with respect to the particle distributions for fixed mass number A , EOS parameters (n_0, w_0, S_0, K_0, L), and gradient coefficient F_0 .

2. Fitting to empirical masses and radii of stable nuclei Ref. Oyamatsu & Iida, PTP **109** (2003) 631.

obtain the EOS parameters for various sets of (K_0, L) by fitting the calculated optimal values of charge number Z , mass, and rms charge radius R_c to empirical data for stable nuclei ($25 \leq A \leq 245$) on the smoothed β stability line.





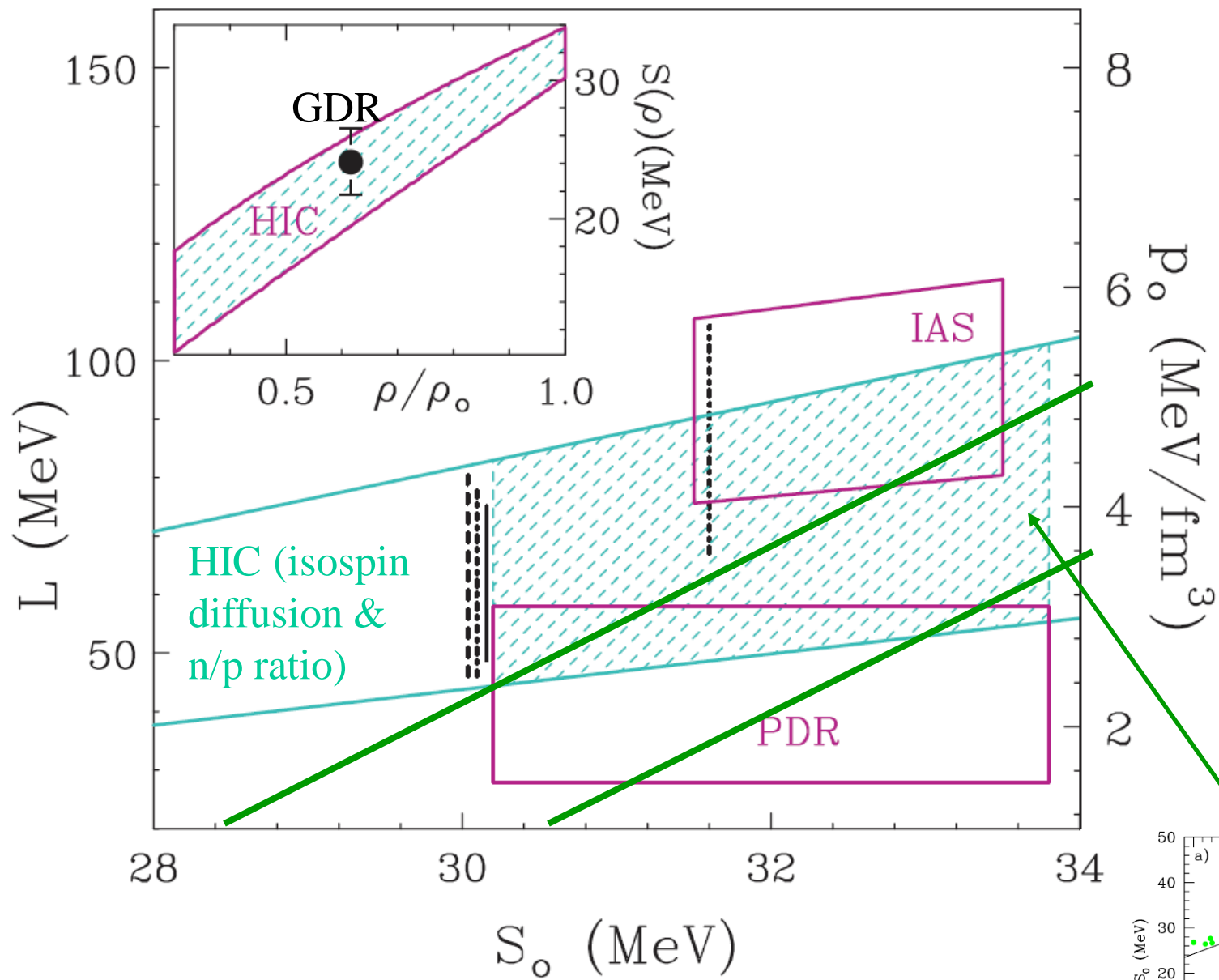
+ from fitting to empirical
masses & radii of stable nuclei

● Skyrme Hartree-Fock models

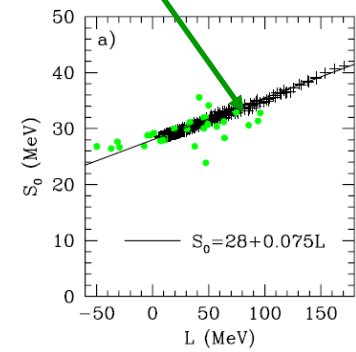
□ SIII

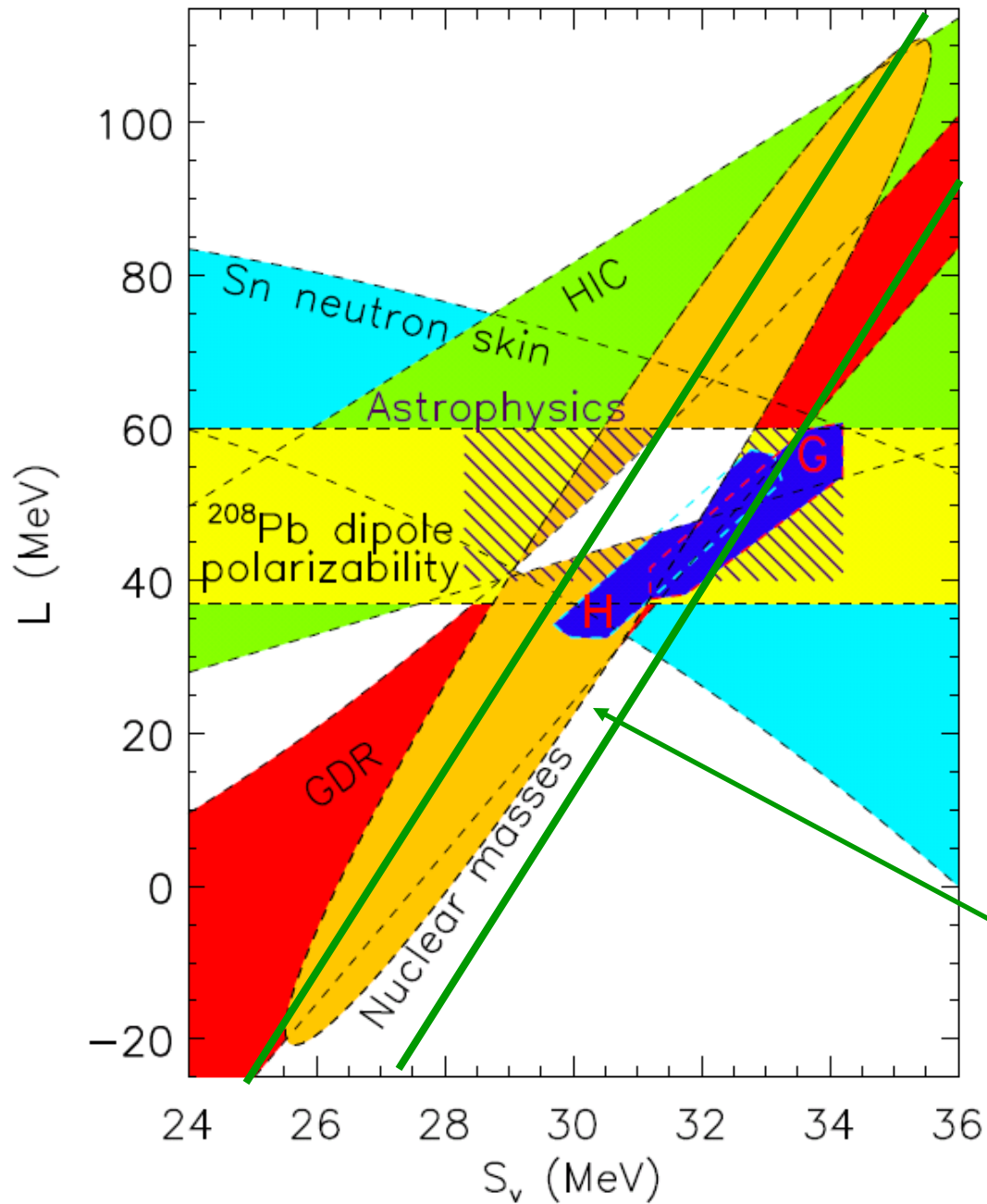
△ TM1

Ref. Oyamatsu & Iida, PTP **109**(2003)631.

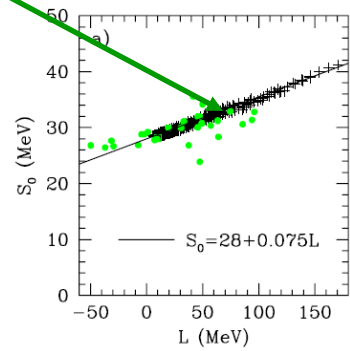


Ref. Tsang et al., PRL **102**(2009)122701.





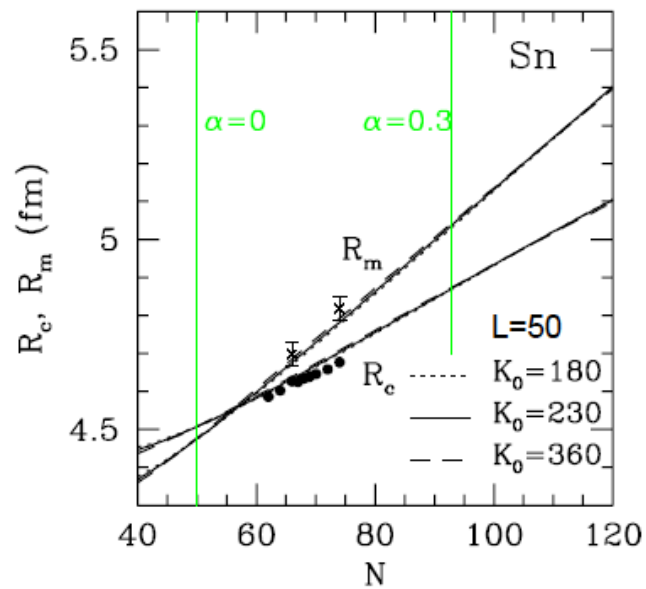
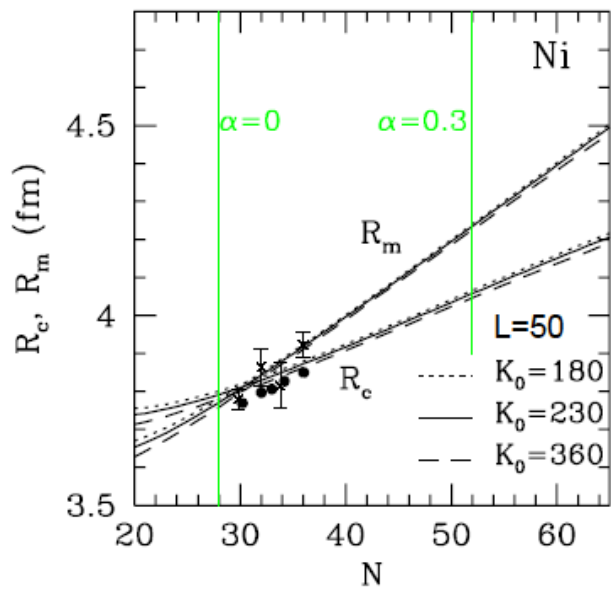
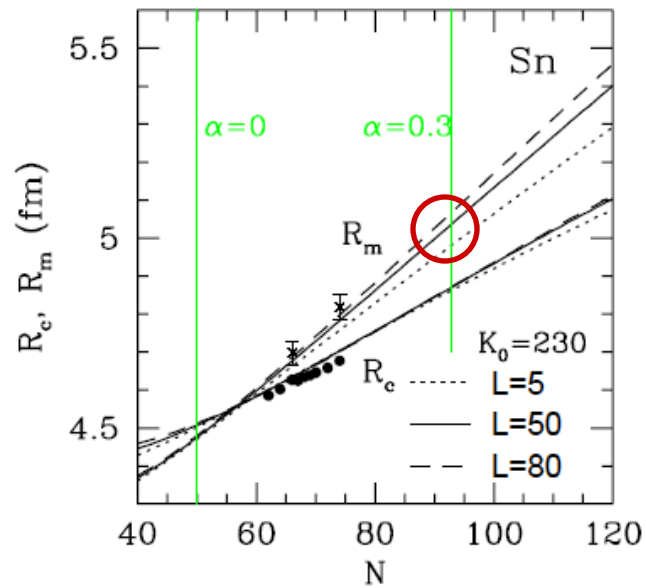
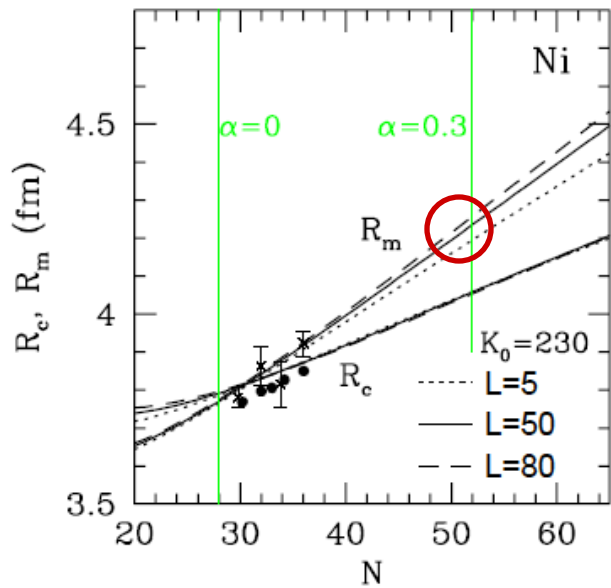
Ref. Lattimer & Lim, arXiv:1203.4286.



Macroscopic nuclear model (contd.)

This model

- good at describing global nuclear properties (e.g., masses, rms radii) in a manner that is dependent on the EOS of nuclear matter
- predicts that the matter radii (R_m) depend appreciably on L while being almost independent of K_0
- not so good at describing the nuclear surface (e.g., diffuseness, skin thickness) in the semi-classical Thomas-Fermi approximation adopted here
- does not allow for shell or pairing effects



Short summary

1. Derivation of the relations between the EOS parameters from experimental data on radii and masses of **stable** nuclei

— L and K_0 are still uncertain.
2. The density-symmetry coefficient L could be determined if a global behavior of matter radii at large neutron excess is obtained from future systematic measurements of matter radii of **unstable** nuclei.
3. The parameter L characterizing the dependence of the EOS on neutron excess is relevant to the structure and evolution of neutron stars in various ways (mass-radius relation, crust-core boundary, cooling, etc.).

Nuclear masses and the equation of state of nuclear matter

Question

Are existing data for masses of unstable nuclei useful for determination of L ?

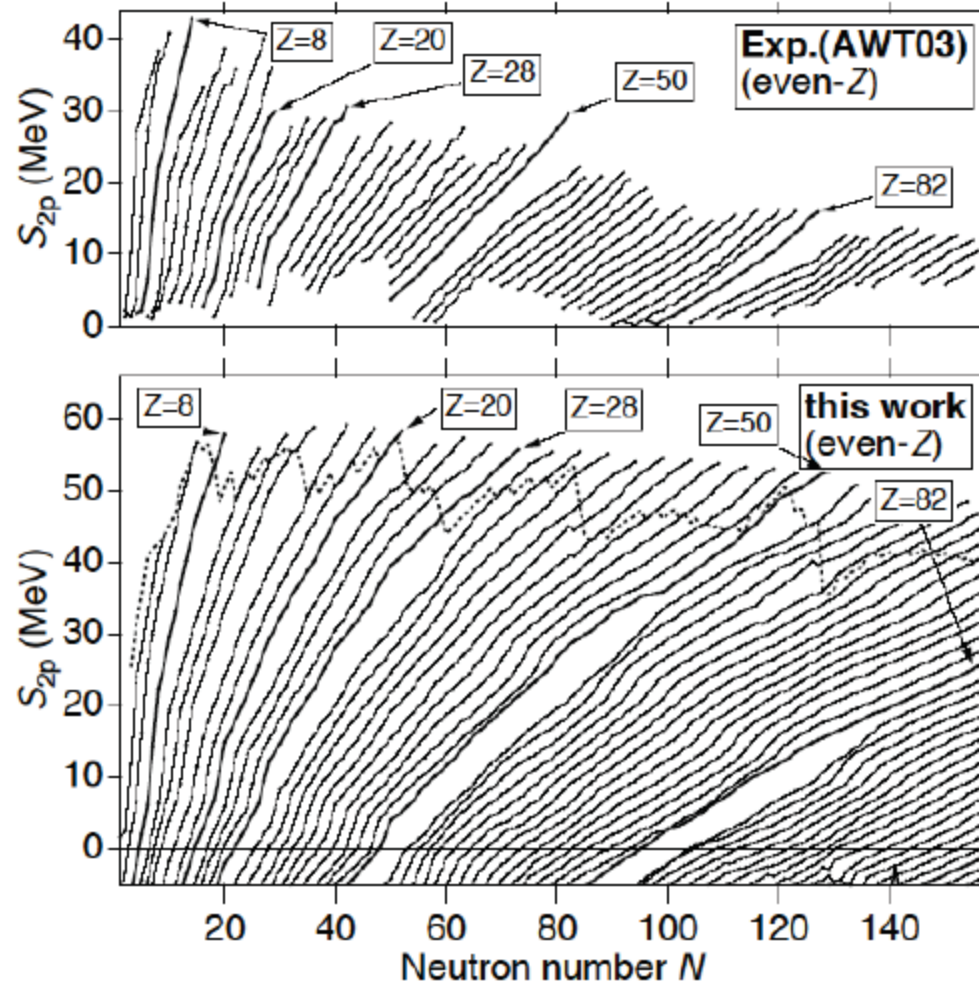
Contents

Two-proton separation energy

L dependence of nuclear masses

L dependence of the neutron drip line

Why S_{2p} ?



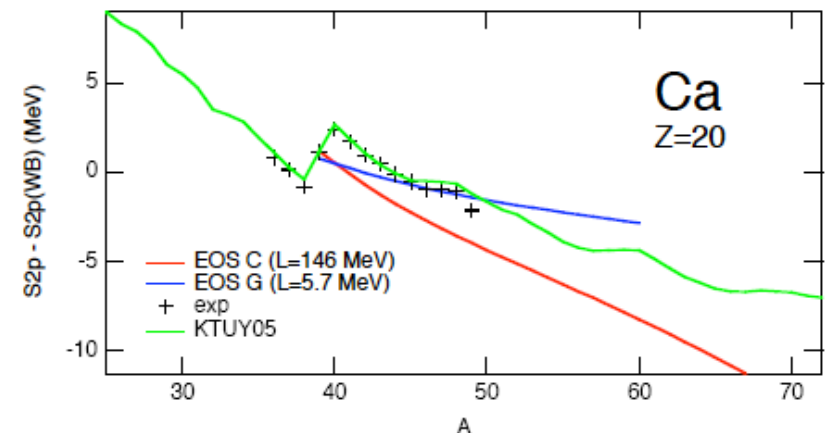
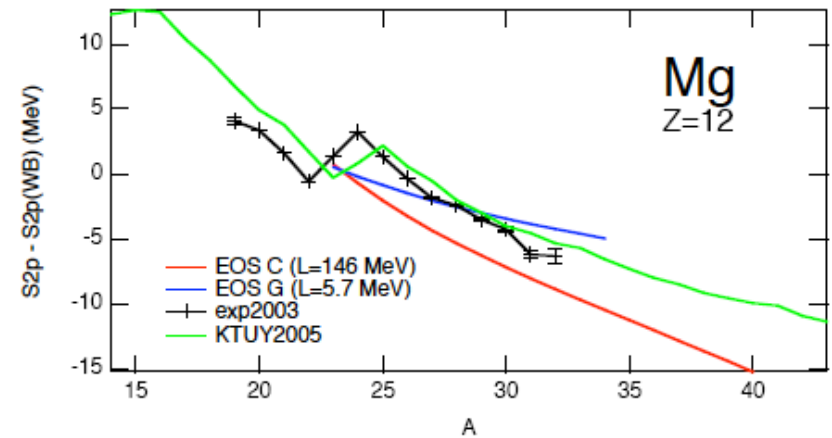
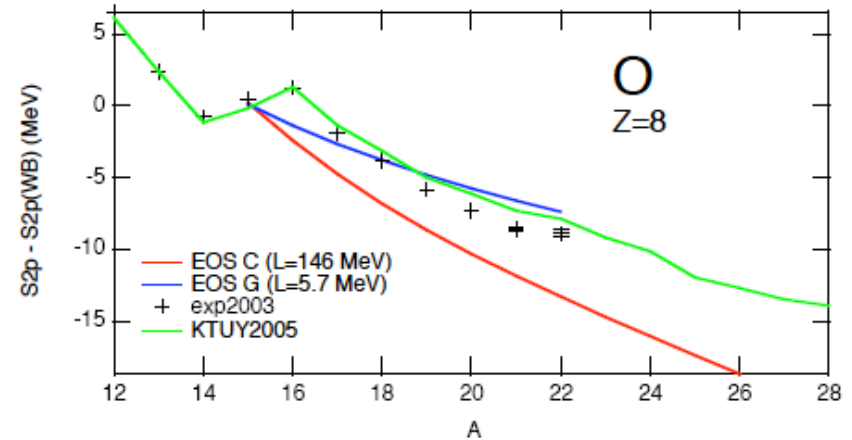
- **Smooth isospin dependence except for shell gaps**
- **Even-odd staggering essentially cancelled out**

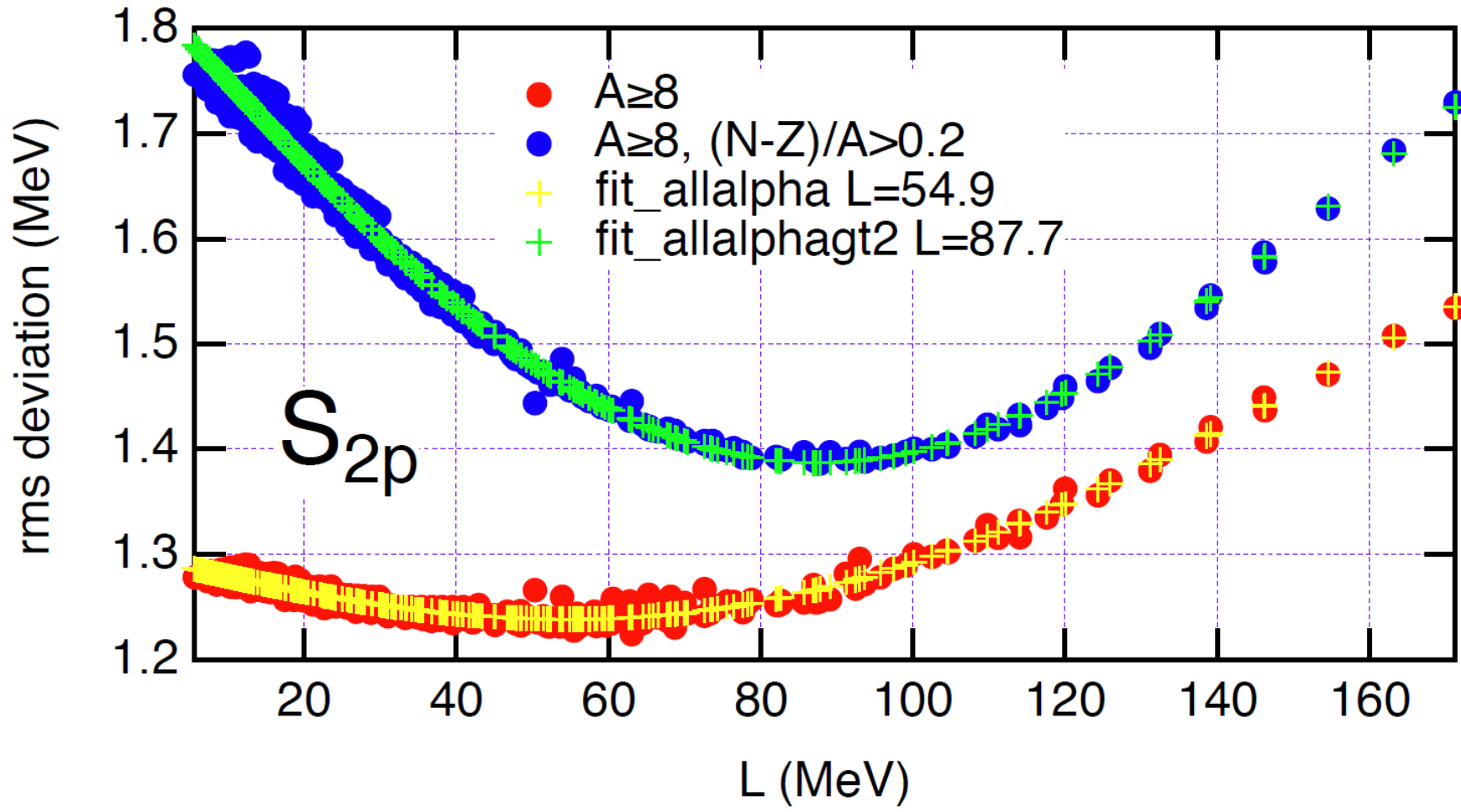
Two-proton separation energy (contd.)

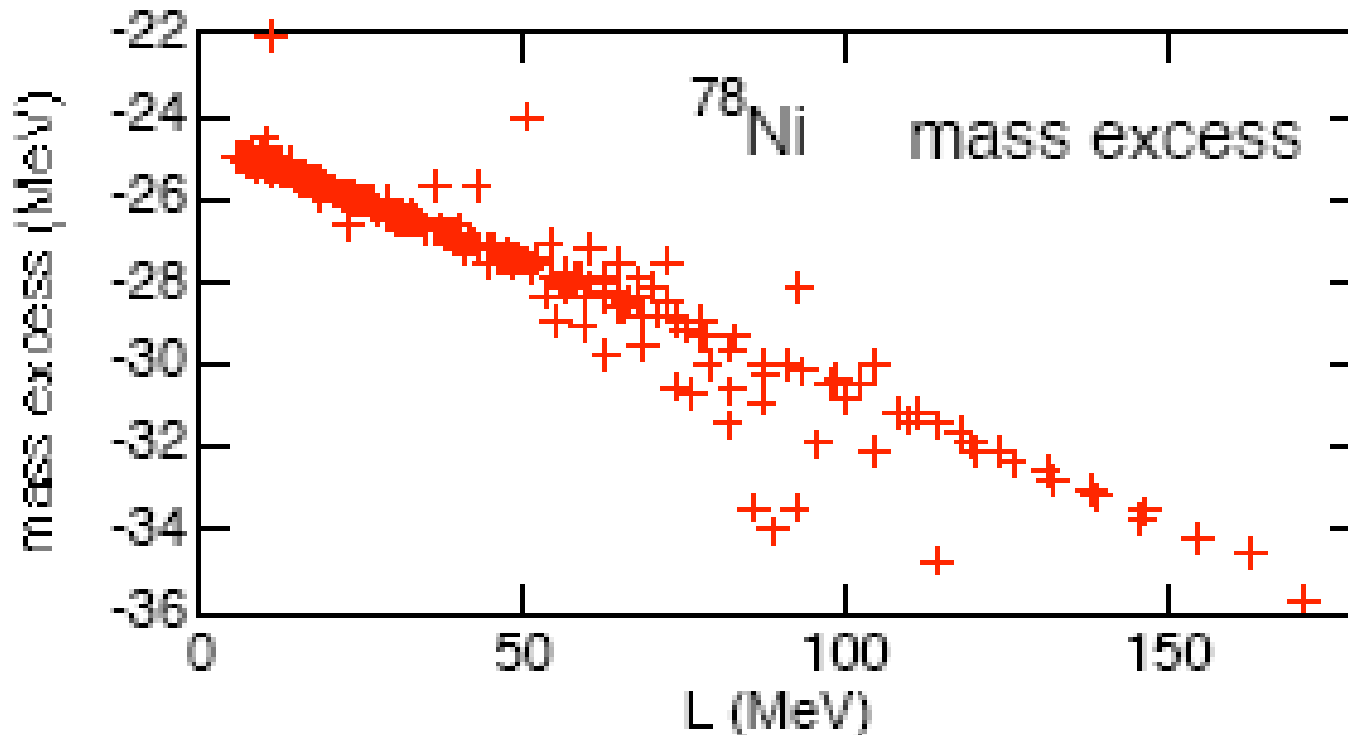
Comparison

- The empirical S_{2p} shows a smooth dependence on neutron excess except for the regimes of $N=Z$, magic N 's, and deformation.
- The calculated S_{2p} shows a larger neutron excess dependence for larger L .
- Comparison between the empirical and calculated S_{2p} looks easier for smaller mass.
- A larger L is more consistent with the empirical data.

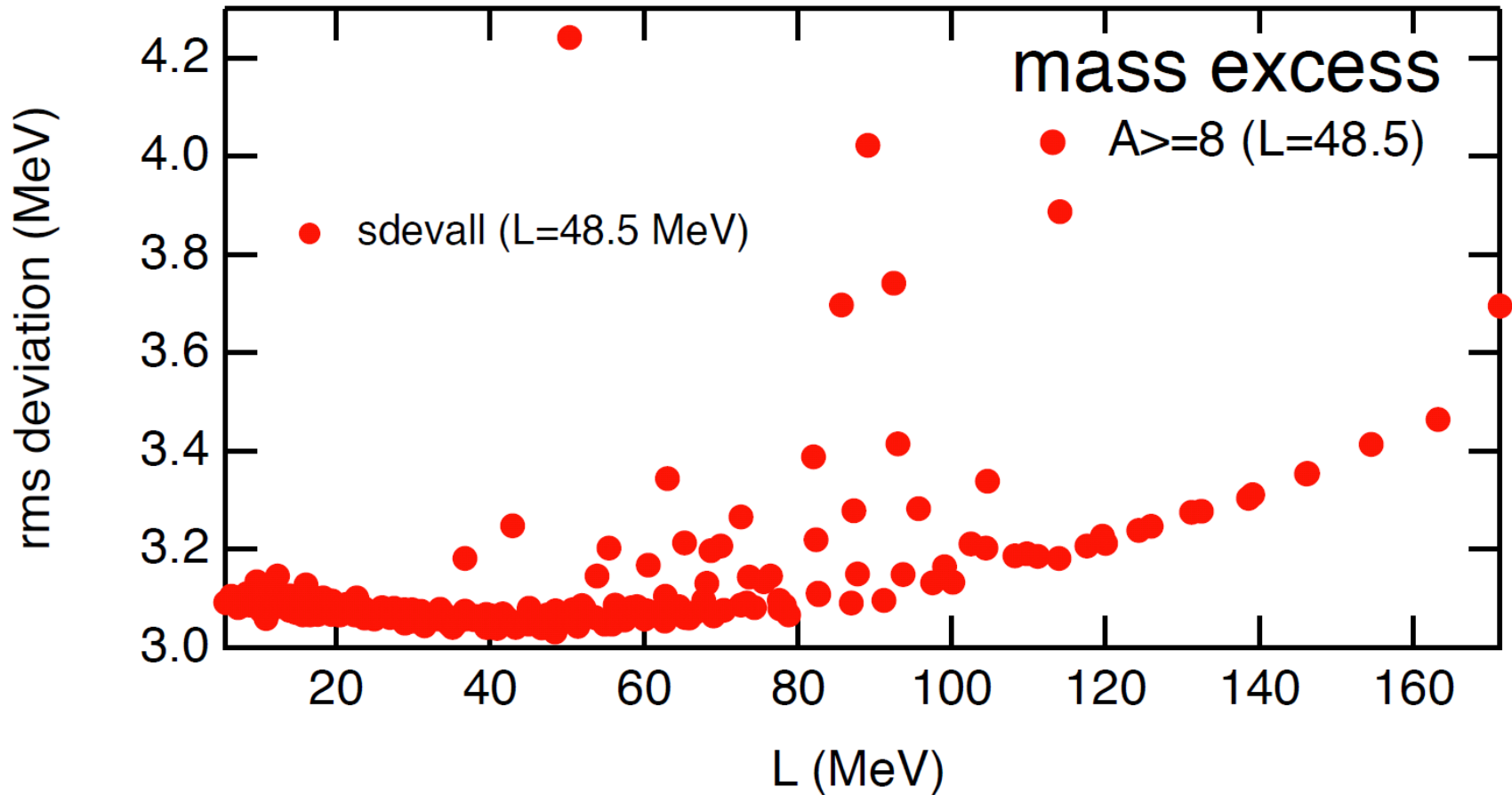
Ref. Oyamatsu & Iida, PRC **81** (2010) 054302.





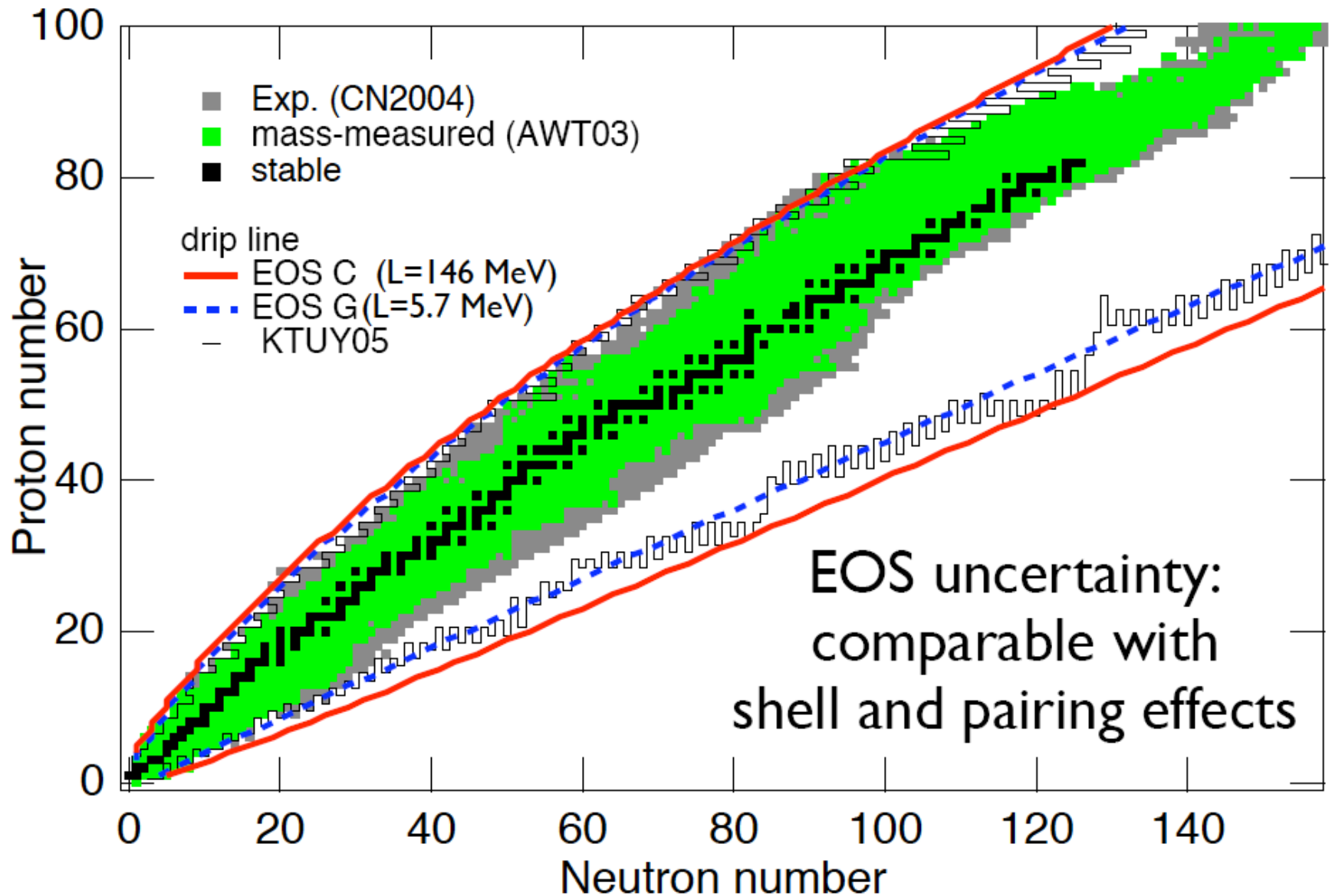


- Nuclear masses are not always dominated by the bulk properties of nuclear matter.
- In fact, the L dependence of the calculated mass cannot be explained by the bulk asymmetry term ($L \uparrow \rightarrow S_0 \uparrow \rightarrow \text{mass} \uparrow$).
- The surface asymmetry term ($L \uparrow \rightarrow \text{surface tension} \downarrow$) is responsible for the L dependence of the calculated mass.



Fitting to mass data for $(N-Z)/A > 0.2 \rightarrow$ optimal L of order 80 MeV

L dependence of the neutron drip line



Neutron star crusts and the equation of state of nuclear matter

Question

Is the presence of nuclear pasta in neutron stars sensitive to the EOS?

Contents

Motivation

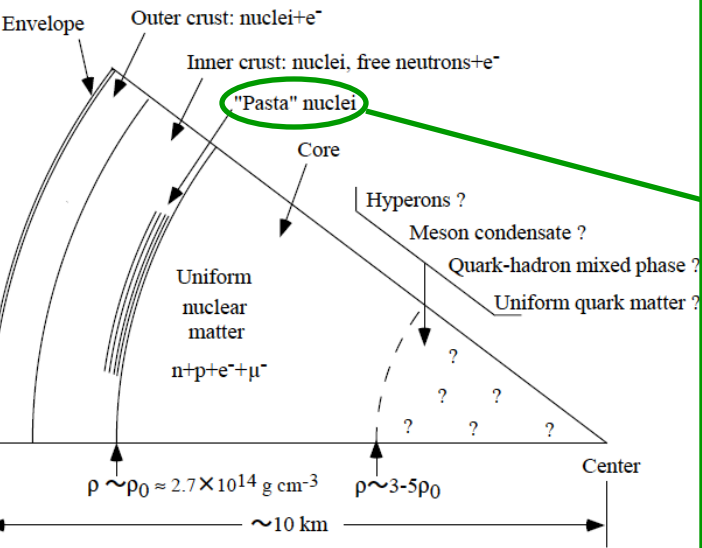
Phase diagrams from macroscopic nuclear model

Gyroid

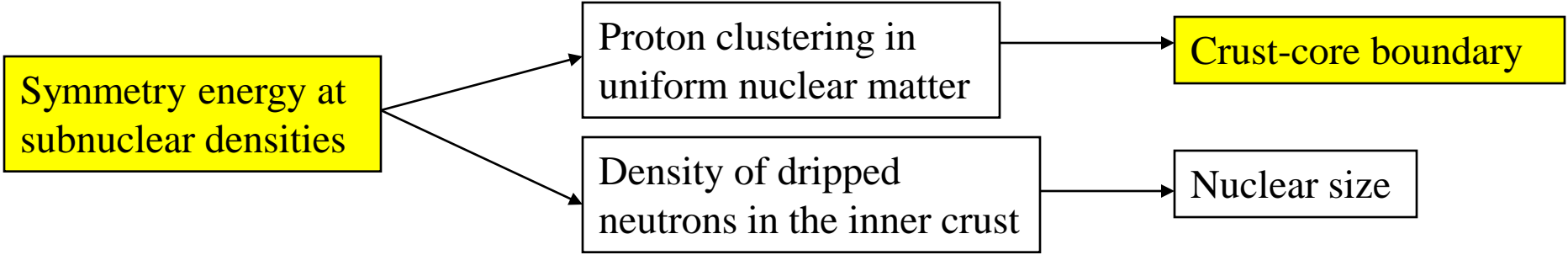
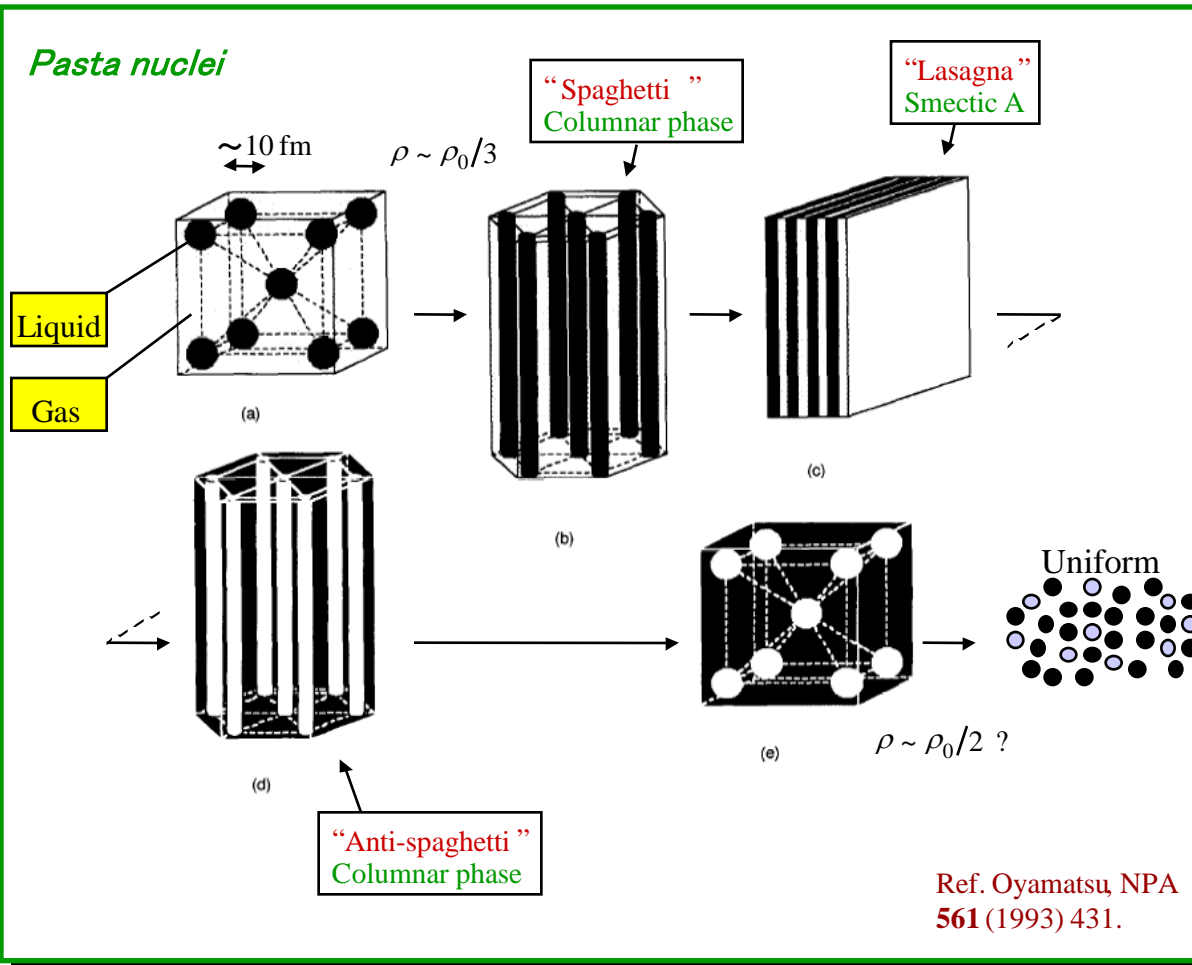
Pastas at finite temperatures

Crustal oscillations

Motivation



Schematic cross-section of a neutron star.



Phase diagrams from macroscopic nuclear model

Macroscopic nuclear model

For a nucleus in vacuum:

Ref. Oyamatsu & Iida, PTP **109** (2003) 631.

$$-E_B = \int d^3r n(\mathbf{r}) w(n_n(\mathbf{r}), n_p(\mathbf{r})) + F_0 \int d^3r |\nabla n(\mathbf{r})|^2 + \frac{e^2}{2} \int d^3r \int d^3r' \frac{n_p(\mathbf{r}) n_p(\mathbf{r}')}{|\mathbf{r} - \mathbf{r}'|}$$

with particle distributions ($i=n,p$):

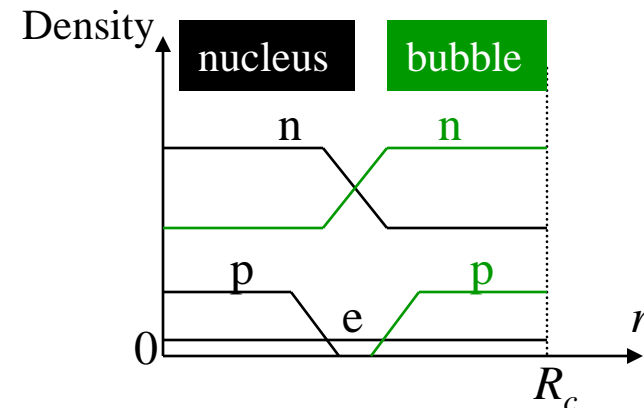
$$n_i(r) = \begin{cases} n_i^{\text{in}} \left[1 - (r/R_i)^{t_i} \right]^3, & r < R_i \\ 0, & r \geq R_i \end{cases}$$

For a nucleus or bubble in a Wigner-Seitz cell:

Ref. Oyamatsu, NPA **561** (1993) 431.

Total energy of a cell: total rest mass $-E_B$ + lattice energy + electron energy

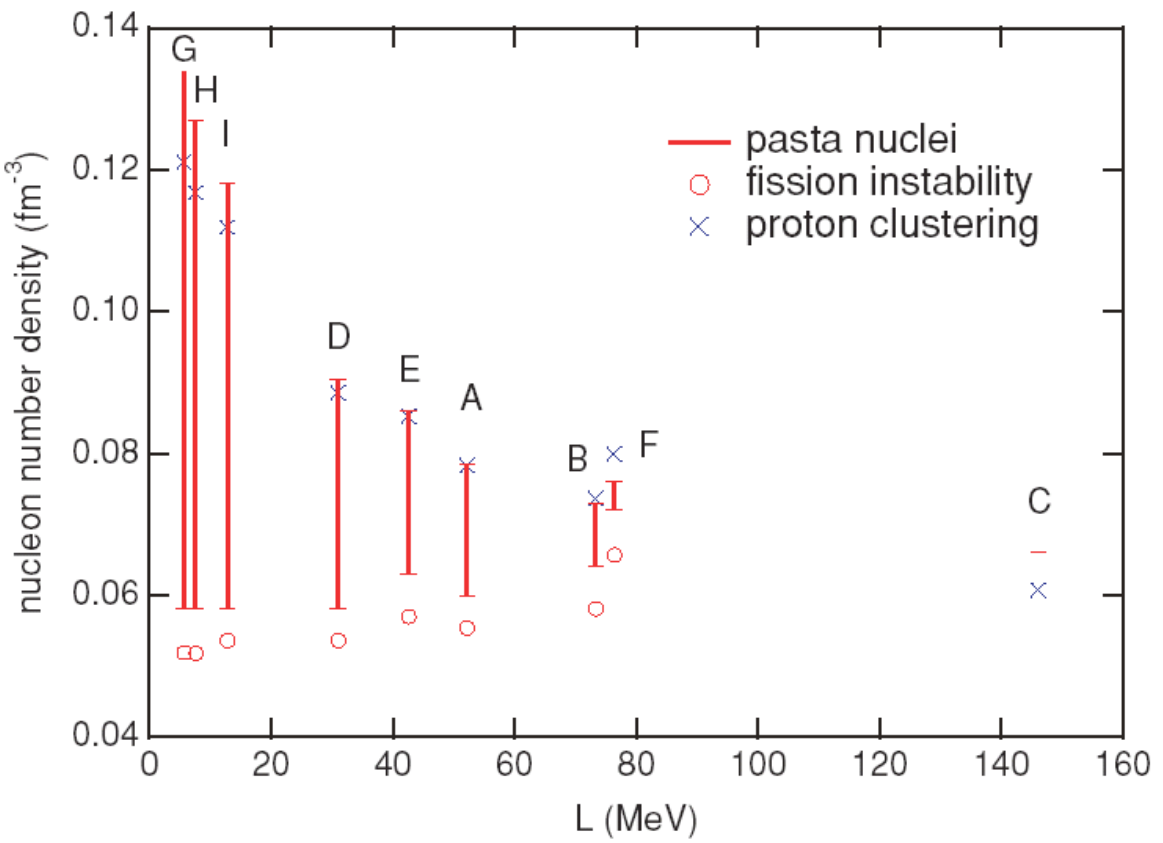
with $n_i(r) = \begin{cases} (n_i^{\text{in}} - n_i^{\text{out}}) \left[1 - (r/R_i)^{t_i} \right]^3 + n_i^{\text{out}}, & r < R_i \\ n_i^{\text{out}}, & r \geq R_i \end{cases}$



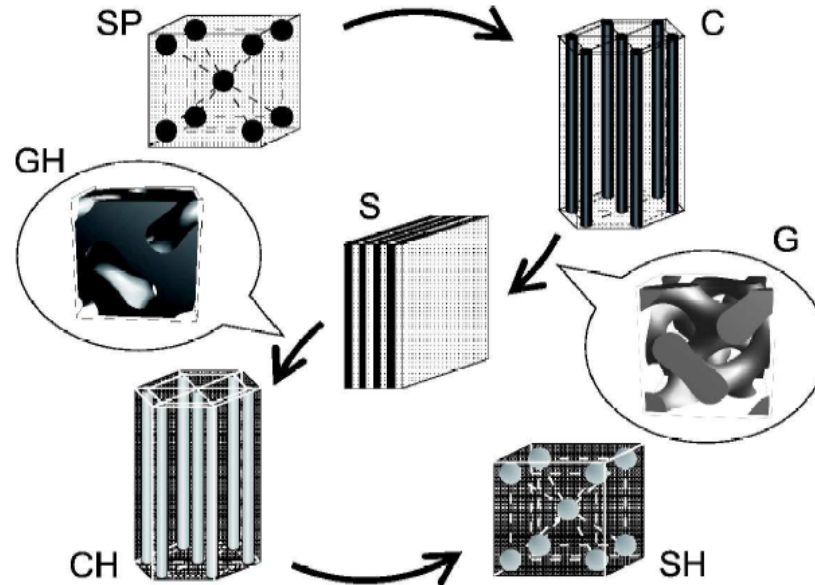
Phase diagrams from macroscopic nuclear model (contd.)

Pasta region

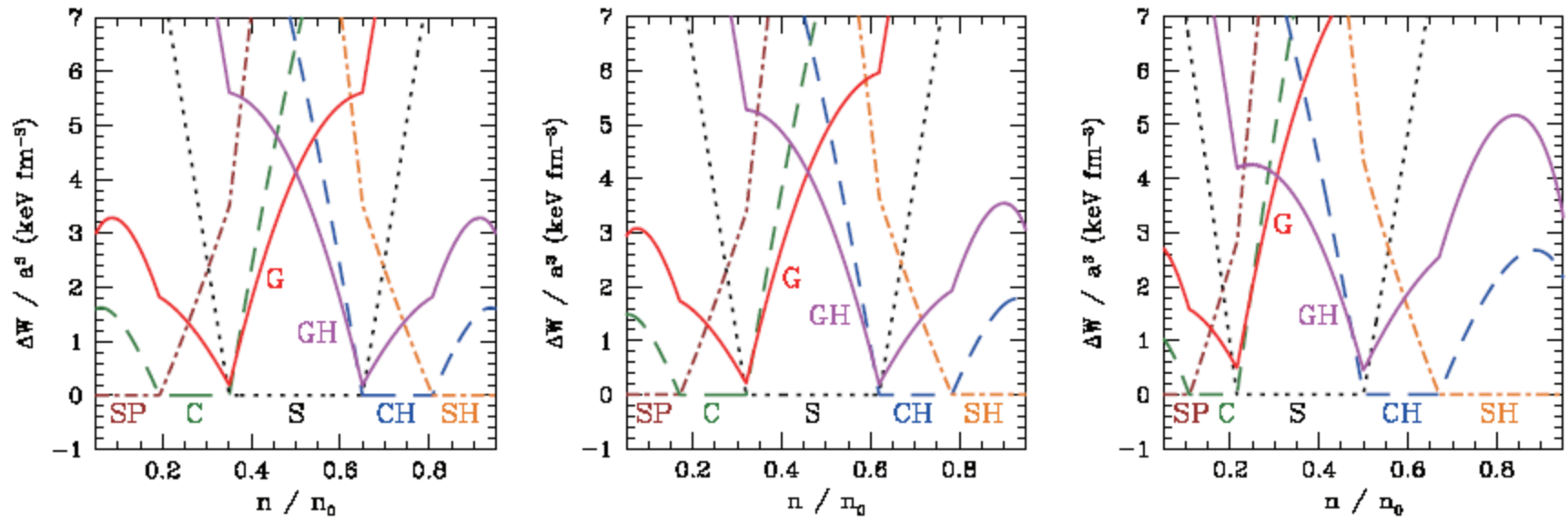
Ref. Oyamatsu & Iida, PRC **75** (2007) 015801.



The larger L , the narrower pasta region.

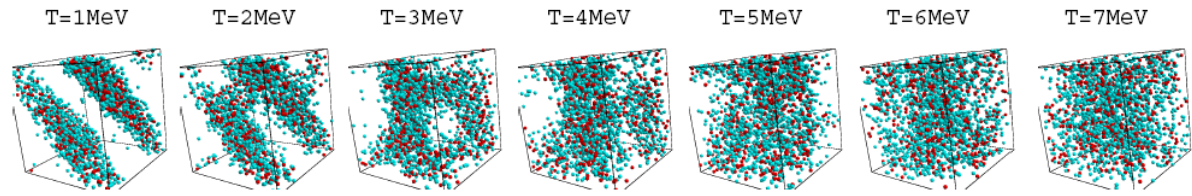


Curvature corrections ($x=0.3$)

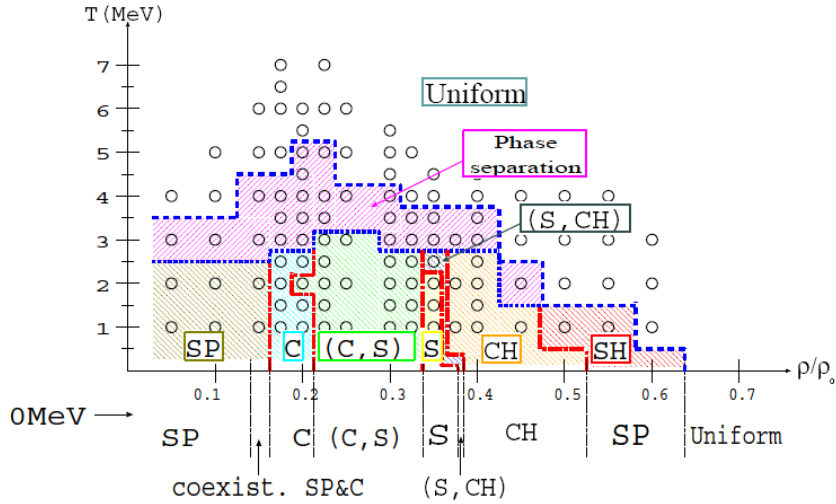


Pastas at finite temperatures

Ref. Sonoda, PhD thesis (2009, U. Tokyo).

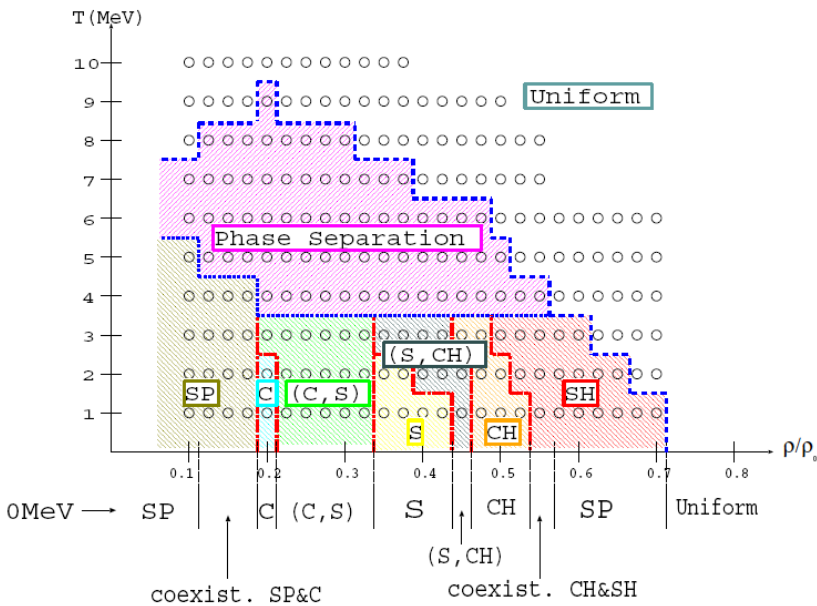


QMD model 1
($L=93$ MeV)



$x=0.3$
 $T < T_c = 15-20$ MeV

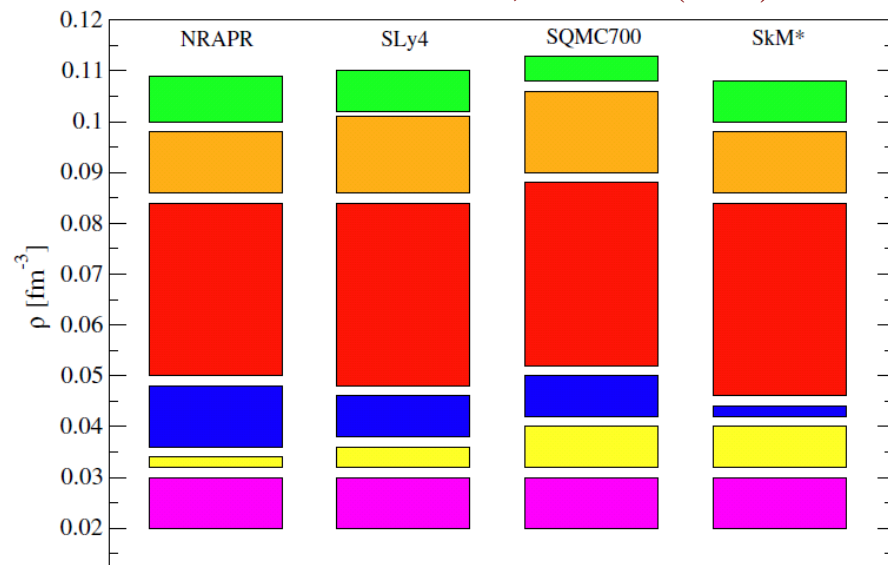
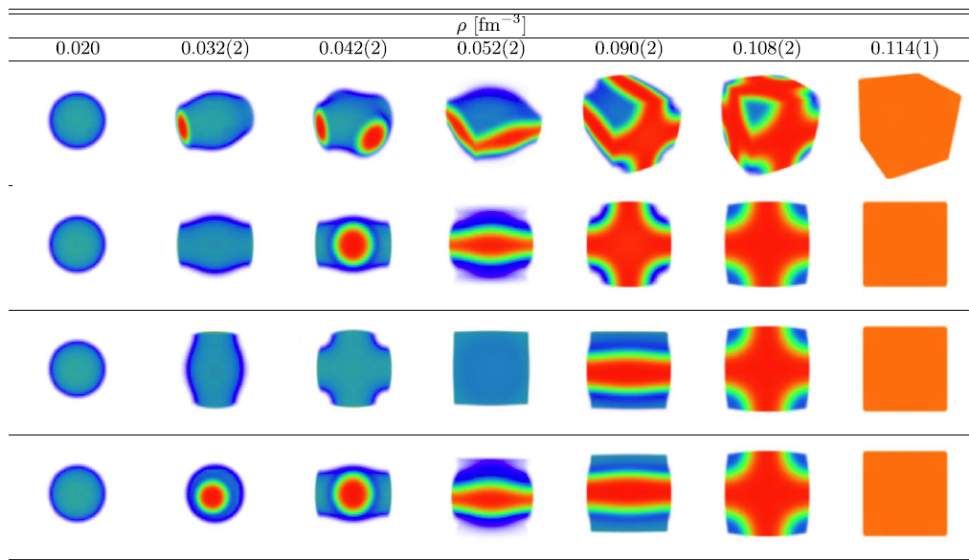
QMD model 2
($L=80$ MeV)



relevant for collapsing
supernova cores

3D HF+BCS ($x=0.3$)

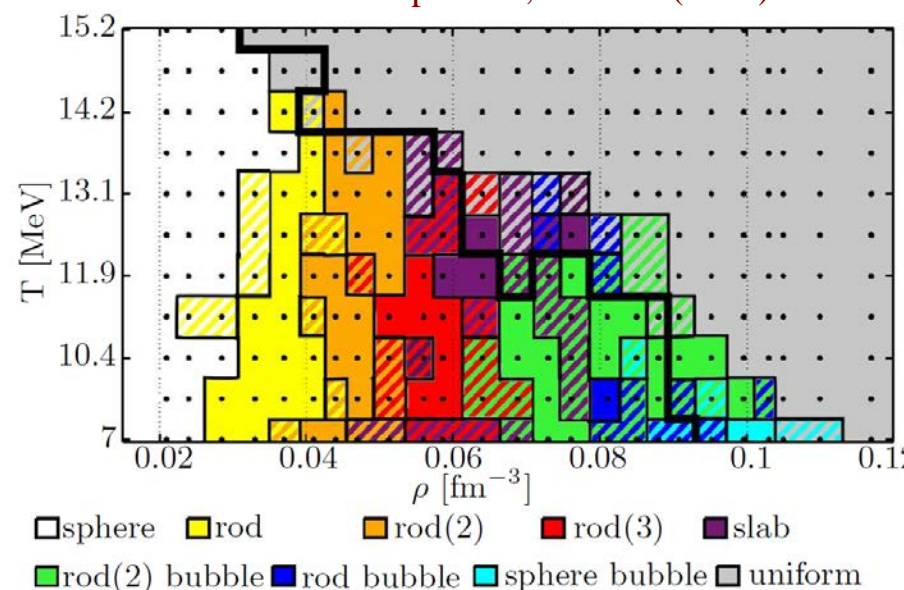
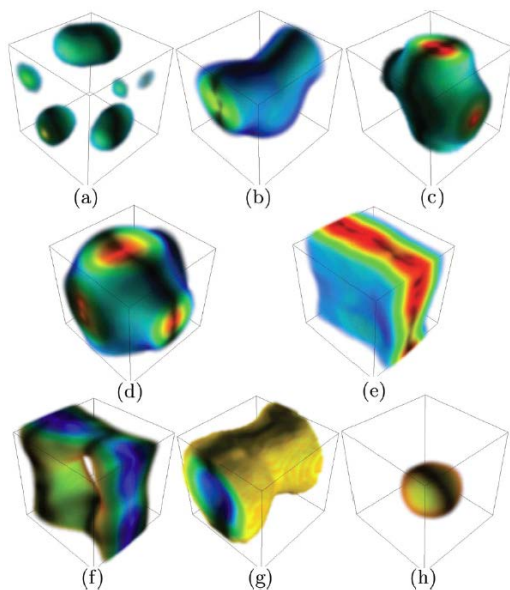
Ref. Pais & Stone, PRL **109** (2012) 151101.



First row: Pasta phases calculated using the SQMC700 Skyrme interaction, $T = 2$ MeV and $y_p = 0.3$.

3D TDHF ($x=1/3$)

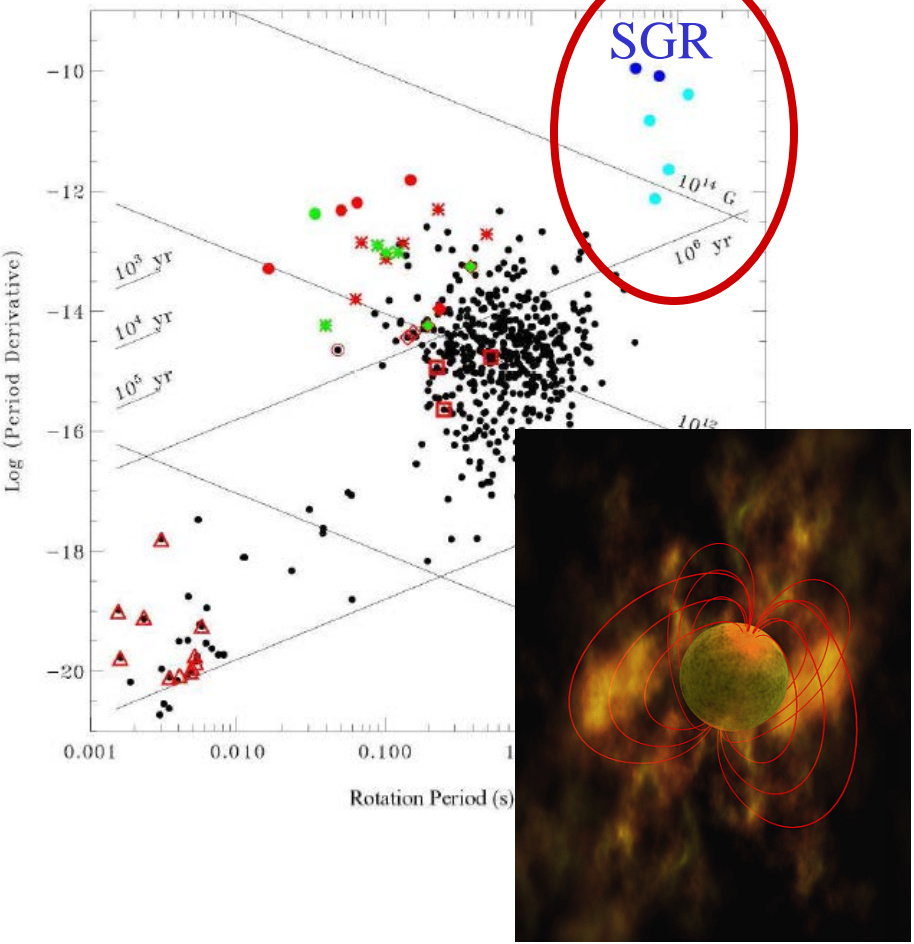
Ref. Schuetrumpf et al., PRC **87** (2013) 055805.



sphere
 rod
 rod(2)
 rod(3)
 slab
 rod(2) bubble
 rod bubble
 sphere bubble
 uniform

QPOs in giant flares from SGRs

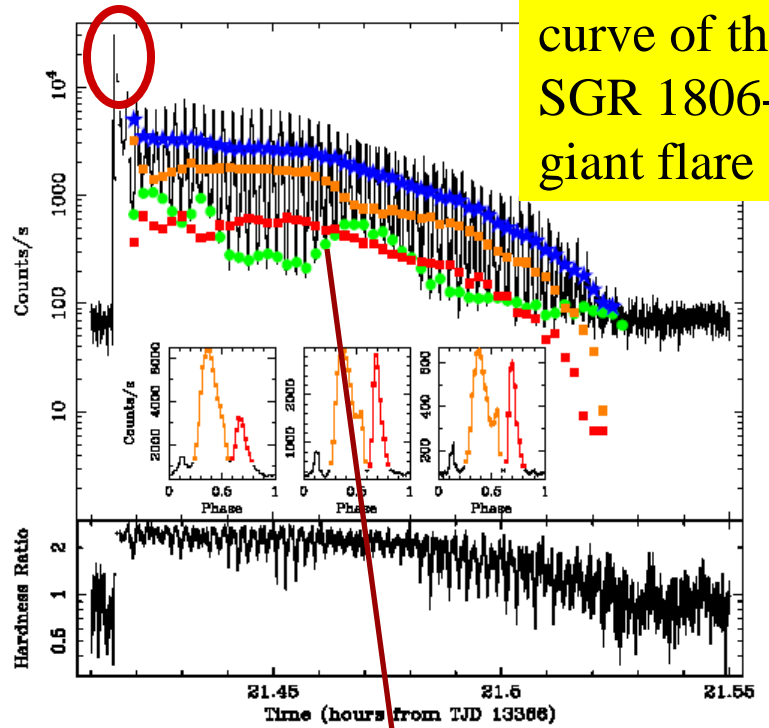
Magnetars



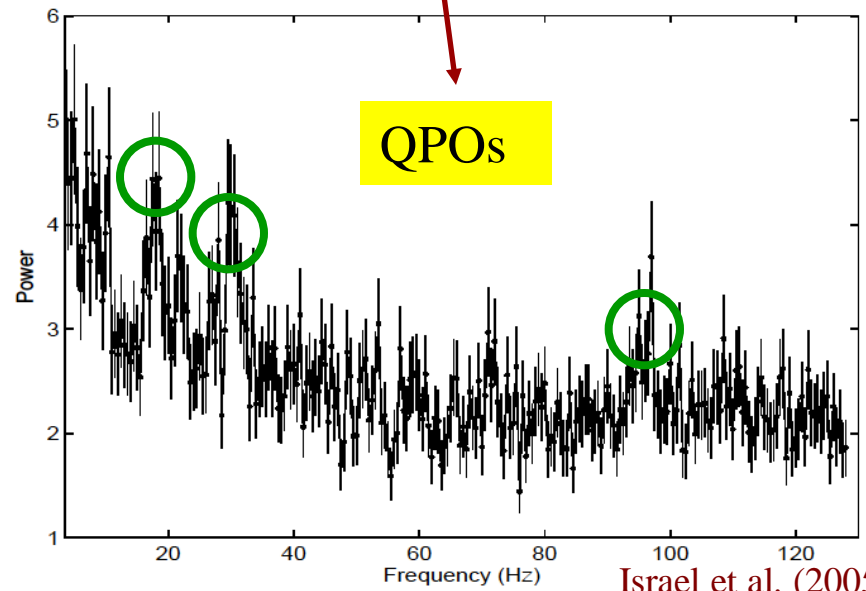
arXiv:astro-ph/0208356

image by NASA

X-ray light curve of the SGR 1806-20 giant flare



QPOs

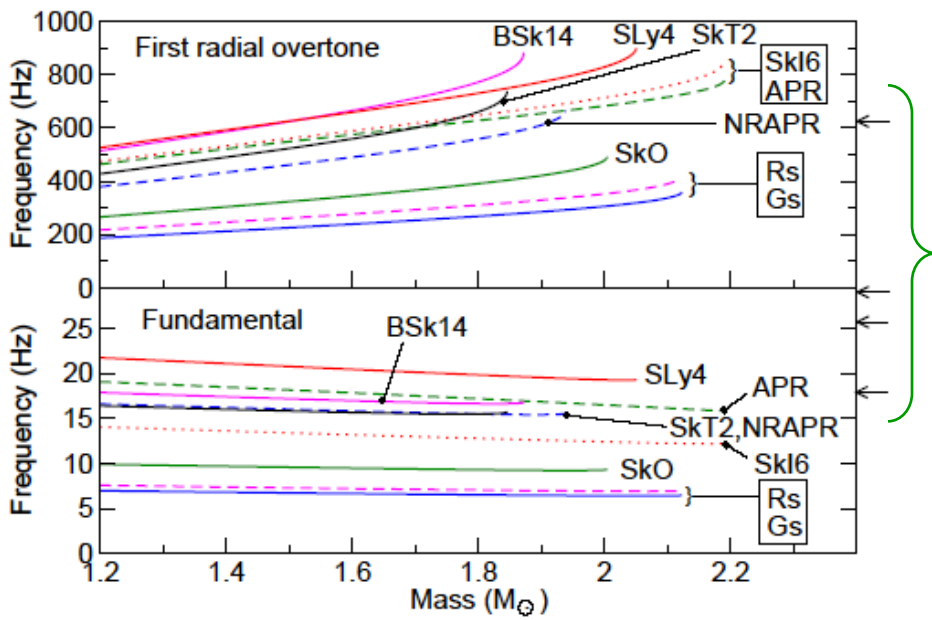
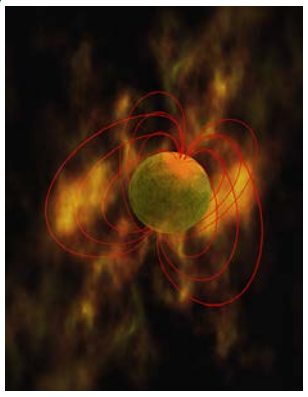


Israel et al. (2005)

QPOs in giant flares from SGRs (contd.)

QPOs in the 2004 giant flare can be identified as crustal shear modes?

If unidentified as shear modes, then Alfvén modes?



Observed QPO frequencies

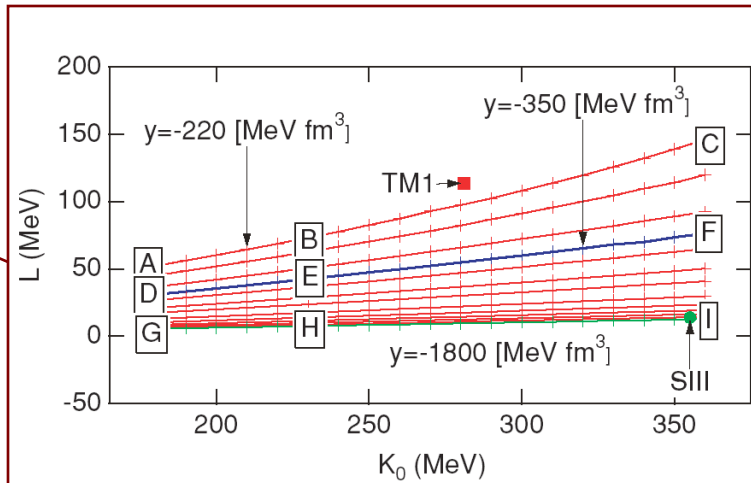
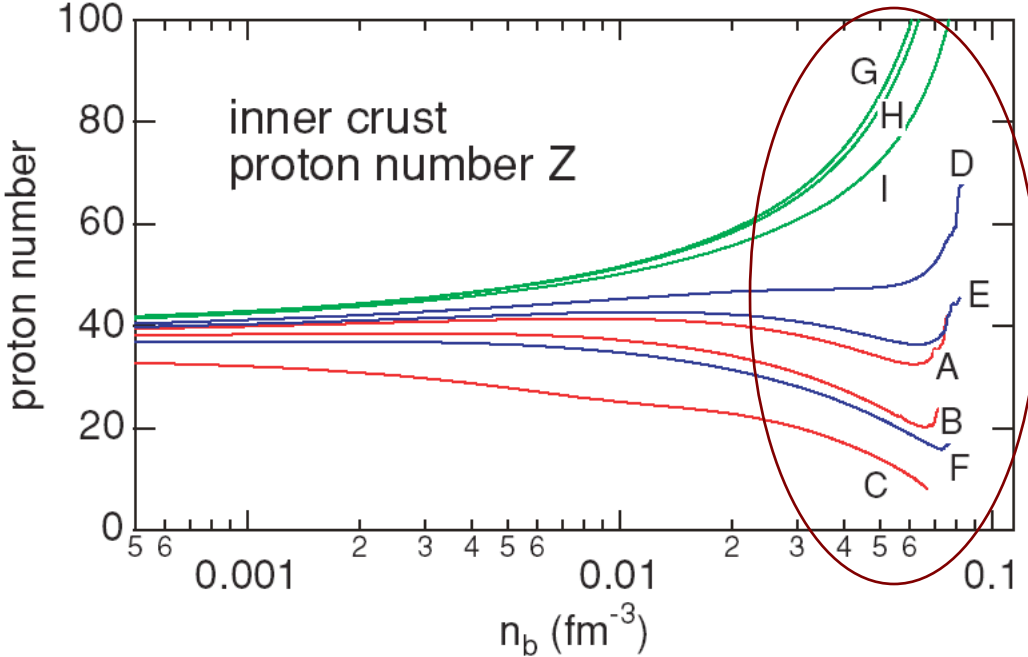
Possible constraint on L via the relation between the shear modulus ($\propto Z^2$) and L !

FIG. 3: The crust oscillation frequencies as a function of neutron star mass, for both the fundamental ($n = 0, l = 2$) torsional shear mode and the first radial ($n = 1$) overtone. The curves end at the maximum mass. The arrows on the right indicate QPO frequencies measured during the 2004 hyperflare from SGR 1806-20 [2, 4, 5].

Steiner & Watts (2009)

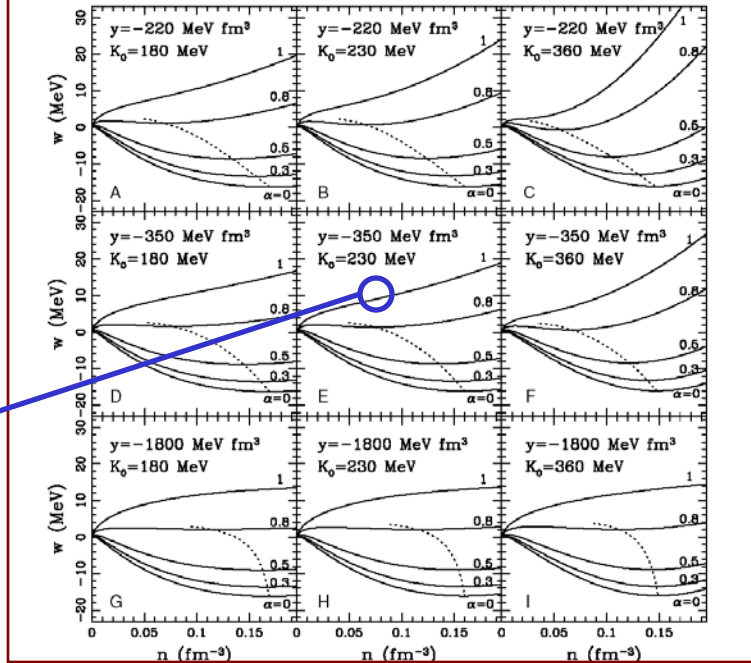
Equilibrium nuclear size in the inner crust of a neutron star

Ref. Oyamatsu & Iida, PRC 75 (2007) 015801.



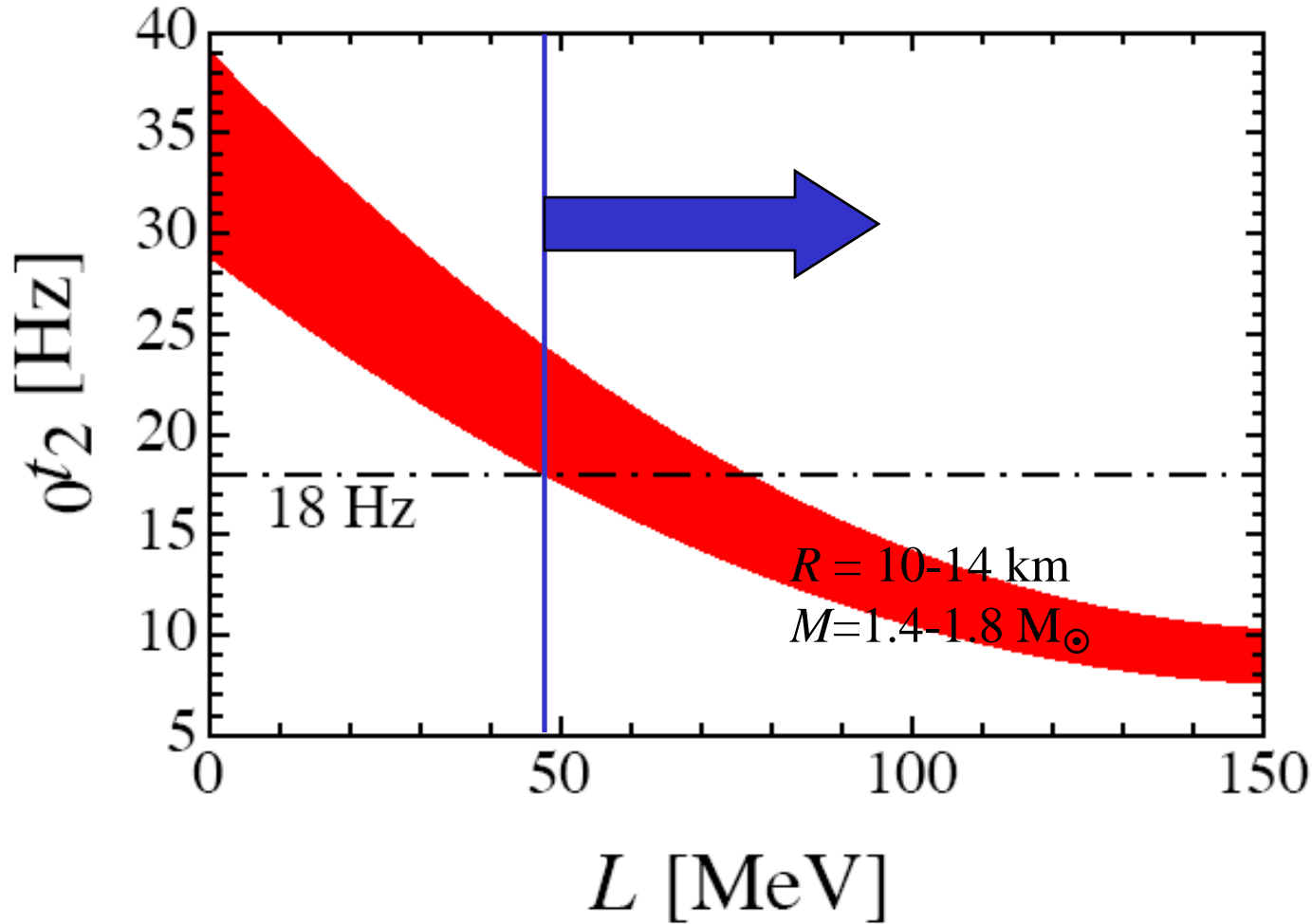
The larger L , the smaller size.

close to the GFMC result with the Argonne v_8' potential

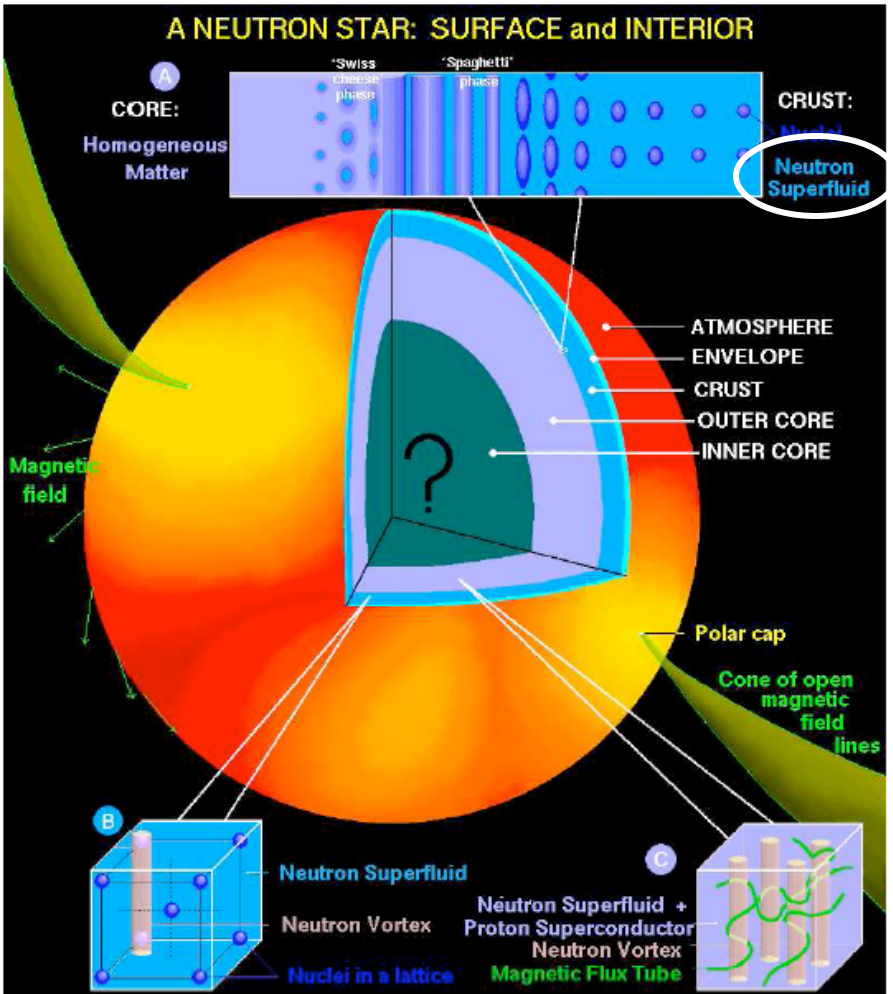


Constraint on L from estimates of crustal torsional oscillation frequencies

Ref. Sotani, Nakazato, Iida, & Oyamatsu, PRL **108** (2012) 201101.



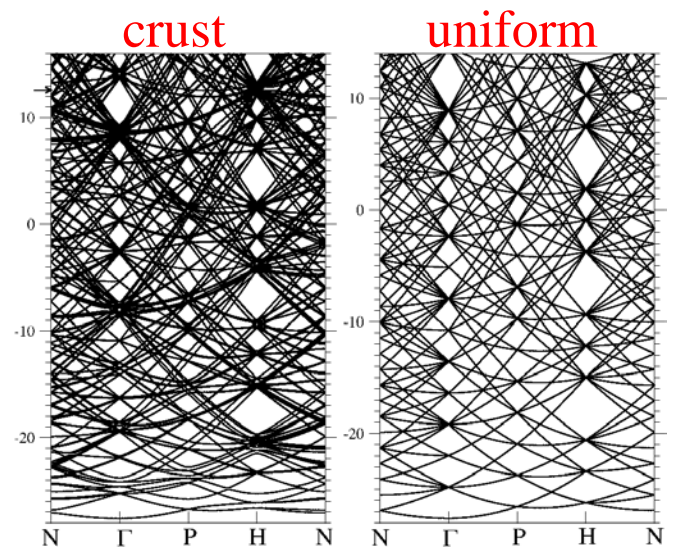
Effects of superfluidity



Lattimer and Prakash, astro-ph0405262

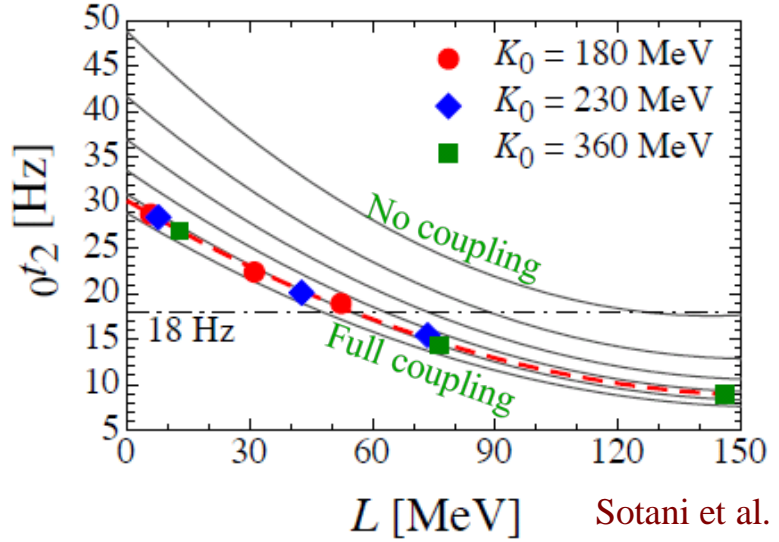
Figure by D. Page

Neutron band structure



Chamel (2012).

Torsional oscillation frequency



Sotani et al. (2012).

Superfluid neutrons are coupled with a lattice of nuclei.

Conclusion

QPOs in giant flares
from SGRs

Pasta region in
neutron star crusts
severely constrained

Nuclear size
in neutron
star crusts

$L > \sim 50$ MeV

Confirmation by Hartree-Fock calculations is desired.